FCP Report No. 42

# THE EFFECT OF SELECTED SUBCYCLES IN BLOCK LOADING FATIGUE HISTORIES

by

Thomas J. Deves
Peter Kurath
Huseyin Sehitoglu
JoDean Morrow

Department of Theoretical and Applied Mechanics

When considering variable amplitude histories representative of service situations, fatigue life estimates employing simple constant amplitude data and a linear damage rule are usually nonconservative. Investigators, in attempts to improve these estimates, have focused their attention on (1) event counting algorithms, (2) alteration of the baseline properties, (3) implementation of other damage summation conventions, or (4) damage criteria (i.e. strain-life, crack growth).

In this investigation, selected variable amplitude histories were chosen, and tests were conducted on smooth cylindrical laboratory specimens. Three methods of analysis were examined, (1) linear damage, (2) plastic work interaction, and (3) J-integral crack growth approach. The results of these analyses and tests are employed to further the understanding of sequence, interaction, and memory effects in fatigue. Results indicate that methods (2) and (3) provide improved fatigue life estimates.

A Report of the
FRACTURE CONTROL PROGRAM
College of Engineering, University of Illinois
Urbana, Illinois 61801

March, 1982

## ACKNOWLEDGMENTS

This investigation was conducted in the Materials Engineering Research Laboratory (MERL) at the University of Illinois, Urbana-Champaign. It was sponsored by the Fracture Control Program, College of Engineering.

The authors wish to thank Todd Christopherson and Bob Goldman for assistance with graphics, and Rene Lara for reduction work and cooperation with publication for this report. Special thanks are accorded Mrs. Darlene Mathine for typing the manuscript.

# TABLE OF CONTENTS


| | Page |
|---|---|
| 1. INTRODUCTION | 1 |
| 1.1 Background | 1 |
| 1.2 Scope | 3 |
| 2. ANALYSIS | 5 |
| 2.1 Basic Concepts | 5 |
| 2.2 Linear Damage | 6 |
| 2.3 Plastic Work Approach | 6 |
| 2.4 J-Controlled Crack Growth Approach | 8 |
| 3. EXPERIMENTAL PROGRAM | 13 |
| 3.1 Baseline Data | 13 |
| 3.2 Variable Amplitude Test Program | 14 |
| 4. DISCUSSION | 16 |
| 4.1 Deformation Characteristics | 16 |
| 4.2 Crack Behavior | 16 |
| 4.3 Fatigue Life Predictions | 17 |
| 5. CONCLUSIONS | 20 |
| REFERENCES | 21 |
| APPENDIX - MEAN STRESS-STRAIN LIFE COEFFICIENTS | 26 |
| TABLES | 28 |
| FIGURES | 43 |

# LIST OF TABLES


| Table | | Page |
|---|---|---|
| 1 | Material Properties | 28 |
| 2 | Cyclic Properties | 29 |
| 3 | Constant Amplitude Strain Controlled Tests (Ramp Waveform) | 30 |
| 4 | Small Crack Measurements from Constant Amplitude Smooth Specimen Replicas | 31 |
| 5 | Strain Controlled Overstrain Tests | 32 |
| 6 | Variable Mean Stress Subcycle Test Results | 33 |
| 7 | Interspersed Varying Mean Stress Subcycle Test Results | 34 |
| 8 | Zero Mean Stress Subcycle Test Results | 35 |
| 9 | Maximum-Mean Stress and Minimum-Mean Stress Subcycle Test Results | 36 |
| 10 | Edited Varying Mean Stress Test Results | 37 |
| 11 | Variable Mean Stress Subcycle Predictions | 38 |
| 12 | Interspersed Variable Mean Stress Subcycle Predictions | 39 |
| 13 | Interspersed Variable Mean Stress Subcycle Predictions | 40 |
| 14 | Zero Mean Stress Subcycle Predictions | 41 |
| 15 | Edited Variable Mean Stress Subcycle Predictions | 42 |

# LIST OF FIGURES


| Figure | | Page |
|---|---|---|
| 1 | Specimen Dimensions and Processing . . . . . | 43 |
| 2 | Crack Length Data . . . . . | 44 |
| 3 | Photos of Acetate Replicas of Specimen 35A Showing Fatigue Cracks . . . . . | 45 |
| 4 | Schematic Illustration of (a) Varying Mean Stress Test and (b) Interspersed Varying Mean Stress Test . . . . . | 46 |
| 5 | Schematic Representation of (a) Max Mean Stress Test, (b) Zero Mean Stress Test, (c) Min Mean Stress Test . . . . | 47 |
| 6 | Experimental Data . . . . . | 48 |
| 7 | Comparison of Constant Amplitude and Overstrain Fatigue Tests | 49 |
| 8 | Predictions and Experimental Results for the Varying Mean Stress Tests . . . . . | 50 |
| 9 | Predictions and Experimental Results for the Zero Mean Stress Tests . . . . . | 51 |
| 10 | Life vs. Initial Plain Cycles in Edited Varying Mean Stress | 52 |
| 11 | Predicted vs. Experimental (a) Plastic Work Interaction, (b) $\Delta J$ Crack Growth, (c) Conventional Linear Damage . . . . | 53 |

# LIST OF SYMBOLS

| | |
|---|---|
| $a$ | Crack length (mm)* |
| $a_i$, $a_f$ | Initial, final crack length (mm) |
| $b$ | Fatigue strength exponent |
| $c$ | Fatigue ductility exponent |
| $C$ | $\Delta J$ crack growth constant (MPa-mm) |
| $d$ | Stress amplitude-plastic work to failure exponent |
| $D$ | Stress amplitude-plastic work to failure coefficient |
| $da/dN$, $\Delta a/\Delta N$ | Crack growth rate/cycle (mm/cycle) |
| $\Delta a/\Delta B$ | Crack growth rate/block (mm/block) |
| $E$ | Linear modulus of elasticity (MPa) |
| $E'$ | Plane strain, stress modified modulus (MPa) |
| $f(n')$ | Function of strain hardening exponent |
| $F$ | Fracture mechanics geometry function |
| $h$ | Plastic work-cycles to failure exponent |
| $H$ | Plastic work-cycles to failure coefficient |
| $j$ | Summation index |
| $K$ | Monotonic strength coefficient (MPa) |
| $K'$ | Cyclic strength coefficient (MPa) |
| $m$ | $\Delta J$ crack growth exponent |
| $n'$ | Cyclic strength exponent |
| $n$ | Number of cycles/block |
| $N_b$ | Number of blocks to failure |
| $N_f$, $N_c$ | Number of constant amplitude cycles to failures |
| $N_i$ | Initiation life cycles |
| $N_m$ | Number of major cycles to failure |
| $N_p$ | Propagation life, cycles |
| $N_s$ | Number of subcycles/block |
| $N_{sf}$ | Number of subcycles to failure |
| $N_t$ | Total life |
| $R$ | Stress ratio in fatigue |
| $W_f$ | Plastic work to failure (MPa) |

*Units employed throughout the text.

| | |
|---|---|
| $\Delta\varepsilon/2$, $\varepsilon_a$ | Total strain amplitude |
| $\Delta\varepsilon_e/2$ | Elastic strain amplitude |
| $\Delta\varepsilon_p/2$ | Plastic strain amplitude |
| $\Delta\bar{\varepsilon}_p/2$ | Stabilized plastic strain amplitude |
| $J_e$ | Elastic component of J (MPa-mm) |
| $J_p$ | Plastic component of J (MPa-mm) |
| $\Delta J$ | Range of J integral (MPa-mm) |
| $\Delta K$ | Linear elastic cyclic stress intensity (MPa-mm$^{\frac{1}{2}}$) |
| $\Delta\sigma$ | Total stress range (MPa) |
| $\Delta\sigma/2$, $\sigma_a$ | Stress amplitude (MPa) |
| $\Delta\bar{\sigma}/2$ | Stabilized stress amplitude (MPa) |
| $\Delta W_p$ | Plastic work/cycle (MPa) |
| $\varepsilon_e$ | Elastic strain |
| $\varepsilon_f$ | Monotonic fracture ductility |
| $\varepsilon_f'$ | Fatigue ductility coefficient |
| $\varepsilon_{fo}'$ | Fatigue ductility coefficient corrected for mean stress |
| $\varepsilon_p$ | Plastic strain |
| $\sum$ | Summation symbol |
| $\sigma$ | Stress (MPa) |
| $\sigma_f$ | Monotonic fracture strength (MPa) |
| $\sigma_f'$ | Fatigue strength coefficient (MPa) |
| $\sigma_{fo}'$ | Fatigue strength coefficient corrected for mean stress (MPa) |
| $\sigma_{max}$ | Maximum stress (MPa) |
| $\sigma_{min}$ | Minimum stress (MPa) |
| $\sigma_o$ | Mean stress (MPa) |
| $\sigma_y$ | Yield stress (MPa) |
| $\nu$ | Poisson's ratio |

# 1. INTRODUCTION

## 1.1 Background

Fatigue life prediction methods have been refined over a period of years to allow designers to better estimate the longevity of components. Crack formation models (sometimes denoted initiation), commonly associated with smooth specimen behavior, and large crack propagation criterion (1,2) employing fracture mechanics concepts, have been used to characterize a material's cyclic behavior. These data are generally acquired on laboratory specimens, rather than the actual critical location of the component, and methods to correlate these data to the actual member have been developed.

The concept of an elastic stress concentration factor, $K_t$, has been employed to correlate notch and smooth specimen behavior for long lives ($>10^6$). Further investigation revealed that small notches do not have their full theoretical effect in fatigue, and the concept of $K_f$, the fatigue notch factor was introduced (3,4). Topper et al. (5) extended this work to include the finite life region by employing Neuber's rule (6). The appropriate value of $K_f$ was found to depend on the material, geometry, load level, load history, and the definition of failure (specimen separation or some arbitrary crack size). Crack propagation life is generally ignored in these analyses, although this assumption is not always justified (7). Another approach has been to assume some intrinsic flaw size, and employ fracture mechanics concepts to calculate an expected life. No definite demarcation exists between these two methods, although attempts have been made to merge them (8,9).

The desire to analyze variable service histories necessitated the categorization of events, such that damage could be assigned from the constant amplitude baseline data. Range crossing, range mean, range pair, and rainflow counting are common methods employed to reduce complex loading histories. It has been shown that the rainflow method provides the best correlation with smooth specimen data (10), and also for crack growth models (11). An efficient computer algorithm for rainflow counting has been developed by Downing and Socie (12).

Once these events have been identified, and a "damage" assigned, the problem of how to assemble these individual damages into a total life assessment

remains. Miner (13) proposed a linear damage summation,

$$\sum_{j=1}^{n} \frac{n_j}{N_j} = 1 \qquad [1]$$

considering that each event induces damage in direct proportion to its constant amplitude life. A short overview of some other damage criteria is given by Leve (14).

In many service situations the large strain excursion or major cycles are few in number relative to the smaller events. The presence of the major cycle constitutes an "overload" or "overstrain," and the relationship between the larger cycle(s) and smaller cycles produces what is frequently denoted as sequence, interaction, or memory effects. Despite the great amount of work that has been done in this area, no clear explanation has emerged to explain the reduced fatigue lives recorded due to these interactions. Brose et al. (15), have chosen to modify the baseline data, rather than alter the damage accumulation criterion, by performing overstrain fatigue tests. A modification to the slope of the stress-life curve has been proposed by Haibach (16) to account for overstress effects. These methods have enjoyed a measure of success (17), because they tend to assign a greater amount of damage to those events in the long life region.

Investigations by authors such as Dowling (10,17), Socie and Artwohl (18), and Conle (19) have shown that in certain cases current life prediction methods consistently make nonconservative fatigue life estimates (actual lives shorter than predicted). For example, numerous subcycles in variable amplitude histories cause shorter lives than estimated even if overstrain baseline data are incorporated with a linear damage summation convention. Nonconservative life predictions are reported in Refs. 20 and 21 even when the "double linear damage rule" is used. These effects are noted for both smooth cylindrical samples and notched members.

As previously mentioned, smooth specimen testing is often employed to estimate crack formation lives. Hunter and Fricke (22), for an aluminum alloy, and Dowling (23), for a steel, have shown that depending on the definition of an initiated crack, that a considerable portion of the fatigue life can be exhausted propagating a crack. From their data it can be inferred

that low cycle (high stress or strain ranges) fatigue tests spend a shorter portion of their fatigue lives achieving this crack size. Takao (24,25) has shown that a small notch with a low $K_t$ can be employed to initiate a crack, but depending on the stress level the crack may not propagate. Frost (26) has reported similar results for notches with higher $K_t$. Also, it has been shown that conventional crack growth models do not adequately describe short crack behavior, even under constant amplitude loading. El-Haddad and Topper (27) have also observed this phenomenon in notched members.

Most of the aforementioned analyses assume a stable Masing (28) material, that the shape of the hysteresis loop shape is independent of its position in stress-strain space, and that sequence effects are adequately accounted for in the event counting algorithm in conjunction with a linear damage summation. In this procedure certain transition and sequence effects are ignored or assumed to be insignificant, although actual data show that the fatigue life can be significantly shorter than predicted (20).

Four explanations have been forwarded to explain these phenomena.

1) Large strain excursions initiate microcracks earlier in life that are then propagated by the small cycles, causing them to do significantly more damage sooner than would be anticipated in a constant amplitude situation.
2) Cyclic plastic deformation due to the major cycle(s) cause a roughening of the surface of the specimen (29), providing more crack initiation sites for the smaller cycles.
3) Damage does not accumulate linearly (14,21,30).
4) The categorization of an "event" is incorrect, in other words there can be significant interaction effects.

It is felt that before the simple linear damage rule is abandoned, a better understanding of the basic mechanics of material behavior that induces these sequence effects is desirable.

## 1.2 Scope

The present study will attempt to:

1) Reproduce the observed effects (fatigue lives shorter than predicted) on smooth laboratory specimens.

2) Determine the characteristics of histories that cause the detrimental effects.
3) Evaluate two alternate methods of fatigue life prediction and compare them to conventional linear damage, and the experimental data.

Smooth specimens of an ASTM A-36 (1020) steel were used. Completely reversed constant amplitude strain controlled tests on 20 specimens were performed to characterize the strain-life fatigue properties. Five types of variable amplitude strain histories were employed to test 34 specimens. The variable amplitude histories were designed to explore the effects of mean stresses, overstrains, hardening and/or softening behavior, and sequence.

A plastic work interaction model and a smooth specimen $\Delta J$ approach are presented in the ensuing section.

# 2. ANALYSIS

## 2.1 Basic Concepts

Fatigue resistance of metals can be characterized by a cyclic strain-life curve. Smooth specimens tested to failure under fully reversed constant amplitude strain control provide the data for these curves. The relationship between strain amplitude and reversals to failure can be represented in the following form:

$$\frac{\Delta\varepsilon}{2} = \varepsilon_f'(2N_f)^c + \frac{\sigma_f'}{E}(2N_f)^b \qquad [2]$$

To account for the presence of a mean stress, the strain life equation has been modified to the following form:

$$\frac{\Delta\varepsilon}{2} = \frac{\sigma_{fo}'}{E}(2N_f)^b + \varepsilon_{fo}'(2N_f)^c \qquad [3]$$

The coefficients, $\sigma_{fo}'$ and $\varepsilon_{fo}'$, are derived in Appendix I. For a given strain, either of these equations can be solved for life, $2N_f$, via iterative techniques.

For a general life estimation technique, it would be desirable to relate cyclic stress and strain amplitudes. The cyclic stress-strain curves for most metals can be modeled using a Ramberg-Osgood type formulation.

$$\frac{\Delta\varepsilon}{2} = \frac{\sigma_a}{E} + \left(\frac{\sigma_a}{K'}\right)^{1/n'} \qquad [4]$$

An alternate model employs the crack behavior of the material to characterize its resistance to damage, which is often formulated as a power law.

$$\frac{da}{dN} = C' \, \Delta K^{m'} \qquad [5]$$

To account for large scale plastic deformation, Eq. 5 has been revised to the following form:

$$\frac{da}{dN} = C \, \Delta J^{m} \qquad [6]$$

In all analyses a linear damage rule, Eq. 1, is employed. The identification of a damaging event, and the damage criterion differs.

## 2.2 Linear Damage

This analysis implements Miner's original hypotheses (13). An event is considered to be a cycle identified employing rainflow counting. Constant amplitude strain-life data were used to assign damage to each event. The damage from the various cycles within a block were summed, with the inverse being the estimated blocks to failure. Other than mean stress for a sub-cycle, no interaction effects are considered with this method. A desire to have a "benchmark" for comparison was the motivation behind these calculations in this study.

## 2.3 Plastic Work Approach

It has been hypothesized that it is plastic deformation that causes fatigue damage (31), and that perhaps the plastic strains could be used to formulate a damage parameter. Employing plastic strain ranges, and stress ranges obtained from baseline strain-life tests it is possible to assign a plastic work expended during the completion of cycle. The area within a hysteresis loop is considered to be representative of the plastic work per cycle. This area may be approximated by the following equation (32).

$$W_p = \left(\frac{1-n'}{1+n'}\right)\Delta\sigma\ \Delta\varepsilon_p \qquad [7]$$

To assign the plastic work to failure for a given strain amplitude, it is necessary to multiply by the number of cycles to failure.

$$W_f = \Delta W_p\ N_f \qquad [8]$$

For the material considered in this investigation, it was possible to fit the constant amplitude smooth specimen data to a power law.

$$\Delta W_p = H(2N_f)^h \qquad [9]$$

If the exponent in Eq. 9 were equal to minus one ($h = -1$), it would imply that the plastic work to failure is a constant. This is not the case for any structural metals (33).

It is possible to correlate the stress amplitude in terms of the work to failure in a power law form.

$$\sigma_a = D'(W_f)^d \qquad [10]$$

This formulation implies that the plastic work to failure is a function of stress amplitude. Considering a cyclically stabilized material represented by a Ramberg-Osgood stress-strain formulation (Eq. 4), a stress amplitude can be calculated for a given strain amplitude. It should be noted that when using a clip on axial extensometer to measure strain, that an average deformation over the gage section is recorded. For low cycle (high amplitude) tests the plastic strain can be assumed to be uniform, whereas for high cycle fatigue the plastic strains are more localized. For this reason, low cycle fatigue data ($<10^6$ reversals) are fit to Eq. 10 and it is assumed that the extrapolation to longer lives at the critical location is adequate. The exponent, d, in Eq. 10 is a negative number less than one implying the work to failure increases as the stress amplitude decreases.

Service loading is generally random, and periodic overloads may be expected throughout the fatigue life. Failure may occur during one of the overloads, but a considerable amount of fatigue damage may be done by the smaller cycles. If one considers that the largest cycle dictates the plastic work to failure, then the smaller cycles will be more damaging than anticipated from constant amplitude testing. The "damage" required to cause failure at the highest stress level in the sequence, $\sigma_1$, is $D_1$. The relative damage required to cause failure at a lower stress level, $\sigma_2$, is:

$$D_2 = \left(\frac{\sigma_2}{\sigma_1}\right)^d D_1 \qquad [11]$$

The exponent, d, can be interpreted as the material's sensitivity to history of stressing. Expressing the damage due to the major cycle in Miner's form,

$$D_1 = \frac{2n_1}{(2N_f)_1} \qquad [12]$$

and considering the interaction effect presented in Eq. 11, one can identify the damage for a block sequence in the following form (34):

$$\Delta D = \frac{2n_1}{(2N_f)_1} + \sum_{j=2}^{n} \frac{2n_j}{(2N_f)_j}\left(\frac{\sigma_j}{\sigma_1}\right)^d \qquad [13]$$

The inverse of the damage is taken to be the blocks to failure

$$N_b = \frac{1}{\Delta D} \qquad [14]$$

This is not unlike the procedure usually employed for block loading histories, except that we have chosen a block to be an event rather than the individual cycles, and employed plastic work to account for interaction effects. The events in Eq. 13 are identified using rainflow counting. Either conventional strain-life data or a plastic work to failure criterion may be employed to calculate $(2N_f)_j$ for a given strain amplitude.

## 2.4 J-Controlled Crack Growth Approach

An alternate approach to fatigue life estimates based on elastic-plastic fracture mechanics concepts is presented below.

When the plastic zone associated with a crack is small (small scale yielding) compared to the crack length and other geometric dimensions, the stress intensity factor K characterizes the elastic stress-strain field surrounding the crack tip. The small scale yielding concept is the basis of linear elastic fracture mechanics. The resistance of materials to static fracture (35) and fatigue crack growth (1,36) are widely characterized in terms of the stress intensity factors.

Limitations exist when linear elastic fracture mechanics is applied to engineering metals that are capable of large plastic deformation prior to fracture. The K-characterization of crack-tip fields fails when the plastic zone is not small compared to the crack length and other dimensions. Therefore, the behavior of small cracks growing inside plastic zones of notches as well as cracks in smooth specimens can not be characterized using linear elastic fracture mechanics. A more general parameter is required to characterize elastic-plastic crack-tip fields and crack growth.

The J-integral, as introduced by Rice (37), is a path independent line integral and is analogous to strain energy release rate, G, but is based on nonlinear rather than linear elasticity. For small scale yielding, J is

equivalent to G, which is simply related to K. In large scale yielding, J characterizes the elastic-plastic strain fields at the crack tip for ductile materials. This concept has been successfully used as a static fracture criterion for elastic-plastic materials (38). Recently, several investigators used the J-integral to characterize fatigue crack growth rate under elastic-plastic cyclic loading. Cyclic J values were estimated for cracked (39), smooth (23,40,41) and notched specimens (42,43). Some investigators have attempted to combine low cycle fatigue and J-integral concepts (40,41).

The application of the J-integral to the fatigue crack growth process could be objectionable, since the J-integral in the mathematical sense is valid only when the deformation theory of plasticity is valid, which does not permit unloading. Dowling and Begley (39) have interpreted the J-integral in its physical sense rather than the mathematical sense as a measure of the crack-tip elastic-plastic strain fields and applied it to cyclic loading. The cyclic interpretation of J is equivalent to the elastic-plastic work required to open crack surfaces. The good correlations obtained between da/dN, crack growth rate, and $\Delta J$ over a wide range of tests proved that the approach taken was promising. A life prediction procedure that characterizes crack growth as the dominant damage mechanism is presented in this section.

An exact J-solution for a smooth specimen is not presently available. Therefore, an estimate will be made. For a material that obeys a Ramberg-Osgood type relationship, Eq. 4 can be employed to represent the stress-strain response of the material. The J-integral can be estimated as a sum of linear elastic and fully plastic contributions.

$$J = J_e + J_p \qquad [15]$$

The elastic portion, $J_e$, can be obtained from linear elastic fracture mechanics,

$$J_e = \frac{K^2}{E'} \qquad [16]$$

where $E' = E$ for plane stress and $E' = E/(1-\nu^2)$ for plane strain. For a semi-circular surface crack of depth a, K is given (44) below:

$$K = 1.12 \frac{2}{\pi} \sigma\sqrt{\pi a} \qquad [17]$$

Here, 1.12 is the free surface correction factor and $2/\pi$ is the correction factor for an embedded crack.

The plastic portion of J, $J_p$, can be estimated from Shih and Hutchinson's (45) work where they analyzed an infinite plate subjected to remote tension.

$$J_p = F\,\sigma\,\varepsilon_p\,f(n')a \qquad [18]$$

Assuming that the correction factor for the linear elastic case applies to the plastic case, we can write:

$$J_p = \left(1.12\,\frac{2}{\pi}\right)^2 \sigma\,\varepsilon_p\,f(n')a \qquad [19]$$

The complete J-integral estimate assuming plane stress when applied to fatigue becomes:

$$\Delta J = 0.51\frac{(\Delta\sigma)^2}{E}\,\pi\,a + 0.51\,\Delta\sigma\,\Delta\varepsilon_p\,f(n')a \qquad [20]$$

An estimate similar to Eq. 20 is obtained by Mowbray (40,41) and Dowling (23). These investigators expressed the elastic and plastic terms in Eq. 20 in terms of the remote strain energy density. Assuming that the tensile portion of the cycle is effective in propagating the crack, $\Delta\sigma = \sigma_{max}$ (if $\sigma_{min} \leq 0$) and $\Delta\sigma = \sigma_{max} - \sigma_{min}$ (if $\sigma_{min} \geq 0$). A similar expression to Eq. 20 is used in Ref. 43 to characterize crack growth in notched members. A power law was used to characterize the ASTM A-36 steel tested under completely reversed loading.

In smooth specimens, crack growth occurs under the application of remote stresses and strains in the fully plastic regime. Therefore, the rate of crack growth is controlled by the range in J given as Eq. 20. Fatigue crack growth rates for two cycles with the same $\Delta J$ value are equal. Damage is calculated only for those portions of the cycles above the crack opening load. In this study the crack opening load is taken as zero. Therefore, all the portions of the hysteresis loops that lie above the zero stress level are taken as damaging. No distinction is made between Stage I and Stage II crack orientations and both are assumed to be controlled by the $\Delta J$ expression given as Eq. 20.

For constant amplitude loading the crack growth rate per cycle can be written as:

$$\Delta a \simeq \frac{\Delta a}{\Delta N} = C(\Delta J)^m \qquad [21]$$

The crack growth rate for variable amplitude block loading can be obtained by adding the crack extension for each cycle within the block (11).

$$\frac{\Delta a}{\Delta B} = \sum_{j=1}^{n} (\Delta a)_j \qquad [22]$$

Combining Eqs. 21 and 22, results in the following form:

$$\frac{\Delta a}{\Delta B} = C \sum_{j=1}^{n} \left[(\Delta J)_j\right]^m \qquad [23]$$

Crack growth rate for the block loading depends on the number of cycles per block and the stress and plastic strain ranges associated with these cycles. When the maximum stress achieved in a block and in constant amplitude cycles are equal the relative crack growth rate can be written as follows:

$$\frac{\Delta a/\Delta B}{\Delta a/\Delta N} = \frac{C \sum_{j=1}^{n} \left[(\Delta J)_j\right]^m}{C[\Delta J]^m} \qquad [24]$$

In arriving at Eq. 24, it is also worth noting that the crack shape and direction should be similar for the block and constant amplitude loading.

$$\frac{\Delta a/\Delta B}{\Delta a/\Delta N} = \frac{\sum_{j=1}^{n} \left[\frac{(\Delta\sigma_j)^2}{E}\pi + \Delta\sigma_j(\Delta\varepsilon_p)_j\ f(n')\right]^m}{\left[\frac{(\Delta\sigma)^2}{E}\pi + \Delta\sigma\ \Delta\varepsilon_p\ f(n')\right]^m} \qquad [25]$$

The stress and plastic strain ranges in Eq. 25 are determined using the cyclic stress-strain curve. If small crack growth increments are considered, the relative crack growth rate is independent of the crack length, the geometry correction factor, and the material constant C. The summation in Eq. 25 employs rainflow counting to identify cycles for a given block.

Inverting both sides of Eq. 25 and integrating both sides from an initial to final crack size, we obtain:

$$\int_{a_i}^{a_f} \frac{\Delta B}{\Delta a}\, da = \frac{\left[\left(\frac{\Delta\sigma}{E}\right)^2 \pi + \Delta\sigma\, \Delta\varepsilon_p\, f(n')\right]^m}{\sum_{j=1}^{n} \left[\left(\frac{\Delta\sigma_j}{E}\right)^2 \pi + \Delta\sigma_j (\Delta\varepsilon_p)_j\, f(n')\right]^m} \int_{a_i}^{a_f} \frac{\Delta N}{\Delta a}\, da \qquad [26]$$

In Eq. 26 the crack initiation length for a block loading and constant amplitude loading is assumed to be equal. Then we have:

$$N_b = \frac{\left[\left(\frac{\Delta\sigma}{E}\right)^2 \pi + \Delta\sigma\, \Delta\varepsilon_p\, f(n')\right]^m}{\sum_{j=1}^{n} \left[\left(\frac{\Delta\sigma_j}{E}\right)^2 \pi + \Delta\sigma_j (\Delta\varepsilon_p)_j\, f(n')\right]^m} N_c \qquad [27]$$

In Eq. 27, $N_b$ denotes variable amplitude loading blocks to failure and $N_c$ denotes constant amplitude cycles to failure. The value of $N_c$ was obtained from the strain-life curve for the corresponding major cycle strain amplitude. Alternatively, $N_c$ could be calculated using Eq. 6 by integrating from $a_i$ to $a_f$. However, the choice of $a_i$ and $a_f$ is somewhat arbitrary. The term on the righthand side of Eq. 27 which is multiplied by $N_c$ is always less than or equal to one for block loading.

Equation 27 was employed for the "crack growth" life predictions made for block loading histories examined in this study.

# 3. EXPERIMENTAL PROGRAM

## 3.1 Baseline Data

The metal tested was ordered as 1020 hot rolled 2" x ¼" x 20' strip stock. Table 1 gives the chemical composition determined from a spectrometer analysis. Smooth specimens were machined from the strip stock to the dimensions shown in Fig. 1. All tests were performed in laboratory atmosphere on an electrohydraulic closed loop testing system under strain control. Strain was measured employing an axial clip on extensometer with a 12.7 mm gage length, except for the high strain tests ($\Delta\varepsilon/2$ = .013 and .015) for which the gage length on both the specimen and extensometer was reduced to 7.6 mm.

Two specimens were used to determine the monotonic tensile properties listed in Table 1 in accordance with ASTM A-370.

Constant amplitude strain controlled fatigue tests, employing a completely reversed triangular wave shape, were performed on 20 specimens. The cyclic properties are summarized in Table 2. Failure was defined as a 50% tensile load decrease from the average tensile peak achieved from cycle 16 through 25. This corresponded to the final crack having propagated approximately 50-60% through the cross section of the specimen. All values for stress and strain were taken from "stable" hysteresis loops (approximately one-half life) (49). Other information on the definition of cyclic stress-strain and strain-life properties can be obtained from Refs. 46 and 47. Five of the constant amplitude tests were monitored for small crack formation employing acetate tape replication procedures (48). The replicas were examined and photographed with an optical microscope, to detect microcracks. Table 3 summarizes these results. A strain-life representation of "crack initiation life" is shown in Fig. 2, where crack initiation is arbitrarily defined as an observable surface crack, with a length of $\sim$.08 mm. A typical set of replica photographs is displayed in Fig. 3.

Overstrain tests as described in Ref. 1 were performed on eight smooth specimens. In the "initial overstrain" tests, ten cycles at ±.01 strain amplitude were applied followed by a ten-cycle incremental step down to zero at the beginning of the test. The desired cyclic strain amplitude was then

applied. The periodic overstrain tests included, in addition to that described for initial overstrain, one cycle at ±.01 (and a ten-cycle step down to zero) every $10^5$ cycles. The failure definition was the same as for the constant amplitude tests.

### 3.2 Variable Amplitude Test Program

The first history to be investigated was one in which a high frequency-low amplitude triangular waveform is superimposed on a low frequency-large amplitude triangular waveform. In stress-strain space this corresponds to sybcycles being "hung" inside the major cycle. This is called the varying mean stress history, and is schematically represented in Fig. 4. One block of data was recorded at logarithmic (i.e.: 1,2,4,8,16,...) intervals.

The second history alternates sets of variable mean stress blocks and plain cycles of equal maximum strain range. A set consisted of logarithmic increments of blocks, and plain cycles (i.e.: 1 block, 1 plain cycle, 2 blocks, 2 plain cycles, 4 blocks, 4 plain cycles, ...) until the limit block/loop sequence is achieved. The test is then continued to failure under the alternating limit block/loop sequence sets. The limit block/loop sequences considered were 50, 100 or 500. It is denoted as the interspersed varying mean stress history and schematically illustrated in Fig. 4. Data were recorded upon the completion of each set. Number of blocks and plain cycles to failure were recorded.

As a comparison, a third type of variable strain history, called the zero mean stress history, that contained the same number of cycles per block with the same amplitude as used in the varying mean stress tests except that the subcycles were applied at zero mean stress, is investigated (see Fig. 5). The zero mean stress history somewhat resembles an overstrain test, but is not exactly the same. These tests were performed with 100, 1000 and 10,000 subcycles per block. Since no step down is employed, the subcycles are located at a nonzero mean strain. For every block, three cycles were recorded, which included the major cycle and the subcycles before and after the major cycle.

Several tests were performed using a variation of the zero mean stress program for which all the subcycles were applied at the maximum mean stress (positive or negative) as in Fig. 5. It was found that for the subcycle strain amplitude and number of subcycles used the mean stress did not relax

completely. Max Mean Stress and Min Mean Stress were the names given to these tests.

Finally, tests were performed with an initial number of plain major amplitude cycles, followed by varying mean stress subcycle blocks to failure. These are called edited varying mean stress tests.

Experimental results for the variable amplitude test program are presented in Tables 6-10.

# 4. DISCUSSION

## 4.1 Deformation Characteristics

The stabilized major cycle and subcycle stress amplitudes in the varying mean stress tests were lower than those observed for the constant amplitude tests at the same strain range. During the varying mean stress blocks of the interspersed varying mean stress tests, the material achieved approximately the same stress levels as observed for the simple varying mean stress tests for both the major cycle and the subcycle. However, hardening occurred during the plain cycles of the interspersed varying mean stress tests, and the stress amplitudes stabilized at approximately the levels observed for constant amplitude loading. This phenomenon was a result of less hardening occurring for a given plastic strain excursion in a varying mean subcycle block rather than being due to a lowering of the yield strength. Stress relaxation due to the presence of mean stress in the subcycles or activation of different slip systems by the subcycles are possible explanations for the observed reduction in overall strain hardening.

The zero mean stress tests displayed minimal differences in stress amplitude for the major cycle when few subcycles ($<10^2$) were involved. With a greater number of subcycles, the major cycle stress amplitude decreased. Again, the subcycle stress amplitude was less than that observed for a similar constant amplitude test, but the deviation was less than that for the varying mean stress blocks. Notably, these conclusions are not evident from the periodic and initial overstrain tests conducted.

The mean stress did not totally relax in the max mean stress and min mean stress tests, although the subcycle stress amplitudes were smaller than a constant amplitude test of comparable strain amplitude, as were the major cycle stress amplitudes. Only four tests of this variety were conducted, so the observations from these tests should be regarded as less decisive.

## 4.2 Crack Behavior

In the variable amplitude tests a tendency for multiple crack nucleation and propagation are observed. Several large cracks (3-4 mm) growing simultaneously near the end of the fatigue life were noted. This is in

contrast to the behavior observed during constant amplitude tests at both high and low strain amplitudes where one dominant crack tends to develop. Multiple crack nucleation is noted for high strain constant amplitude tests, but most of the cracks do not appear to grow, except for the dominant crack. In the varying mean stress, and the interspersed mean stress tests, multiple crack formation and propagation were observed during the subcycle blocks. If multiple cracks were formed during the subcycle blocks of the interspersed varying mean stress tests, they tended to form a single dominant crack when plain cycles ensued.

These observations tend to indicate that the large cycles nucleate multiple cracks, that are propagated by the smaller cycles. Observations by Hunter and Frickie (22), Dowling (23), Ewing and Humfrey (31) and Fig. 2 support the early crack formation postulate for higher amplitude cycles. References 21 and 50 indicate that for variable amplitude loading with larger strain excursions, crack growth may be the dominant damage mechanism. This was the reason the $\Delta J$ type analysis was attempted, and deemed to be appropriate.

## 4.3 Fatigue Life Predictions

Fatigue life predictions for the variable amplitude histories employing (1) linear damage, (2) plastic work interaction, and (3) J-integral crack growth approach are presented in Tables 11-15. Life estimates were calculated for some cases where no tests were performed in order to observe trends of the various prediction methods.

Conventional linear damage predictions for the variable histories considered are always nonconservative. Figure 6 graphically displays the experimental results. If a linear damage analysis were appropriate, the points would lie in the vicinity of the diagonal line. The use of initial or periodic overstrain data in conjunction with linear damage does not account for the reduced fatigue lives in the material tested. Figure 7 suggests that in the finite fatigue life region that this material shows minimal sensitivity to an initial or periodic overstrain. The overstrains may eliminate the "endurance limit", but extrapolation of the strain-life curve seems to be an adequate representation for the baseline data.

Figures 8 and 9 display the experimental results for the varying mean stress and zero mean stress tests along with the trends of the three prediction methods. These plots were deemed appropriate for the unaltered block tests. The plastic work interaction and $\Delta J$ crack growth predictions are more conservative than linear damage. The plastic work interaction model achieved better predictions for the varying mean stress than the zero mean stress tests, though for both cases the estimates are generally conservative. For the varying mean stress tests, the subcycles are "hung" within the major cycle, in other words the subcycles occur before the major cycle is completed. On the other hand, for the zero mean stress tests, the major cycle is completed before the subcycles occur. This was taken to be the major difference between these tests rather than the mean stresses not being identical.

Plastic work interaction assumes the plastic work to failure is dictated by the stress amplitude of major cycle. This appears to be appropriate when the subcycles are "hung" within the major cycle. That the periodic and initial overstrain test results can be predicted reasonably well from a conventional linear damage analysis indicates that the major cycles do not have the interactive effect predicted by plastic work. This indicates that a given number of subcycles following a major event could have an interactive effect. With a large number of subcycles, this effect could decrease as the number of subcycles increases. The zero mean stress tests displayed this phenomenon. Therefore, it seems important to identify exactly what is meant by a "damaging event", which no present scheme adequately achieves.

It should be noted that for a higher strength material which displays a sensitivity to initial or periodic overstrain (15) that the plastic work interactive exponent (Eq. 10) is a larger negative number. This indicates that a harder material may have a diminished interactive sensitivity, but an increased memory of prior completed events. No methods are forwarded by the authors to accomplish this definition of an event. The plastic work interaction and J-integral approach both result in a stress-strain product raised to a power within a summation to incorporate an interactive effect, although the basic assumptions for the two analyses differ.

Figure 10 displays the experimental trends of the edited varying mean stress tests. It shows that the number of initial cycles does not have a large effect on the total fatigue lives. Both the $\Delta J$ crack growth, and plastic

work interaction models predict these observed results well. In both of these models the damage for the initial plain cycles is calculated using Eq. 1, and in all cases this was less than one. The damage per block was then calculated employing either $\Delta J$ or $\Delta W_p$ techniques. It was assumed that, when the damage due to the blocks in addition to the initial damage was equal to one, failure would occur. A similar algorithm was employed for the interspersed mean stress tests, identifying plain cycles and block cycles as separate events when assigning damage, and employing a linear damage summation equal to one to predict failure.

The success of both plastic work interaction, and $\Delta J$ crack growth models in predicting these fatigue lives lends further support that traditional identification of a damaging event is incorrect. Consideration of interaction effects is vital. It should be noted that the experimental trends observed for the edited varying mean stress tests (Fig. 9) were for a major cycle amplitude of .005. Both $\Delta J$ and $\Delta W_p$ approaches do not predict similar results for a major cycle amplitude of .01 (see Table 15).

The max and min mean stress tests show that a compressive mean stress may be beneficial. It should be noted that the zero mean stress tests for similar major cycle and subcycle strain amplitudes display shorter fatigue lives than the maximum mean stress. No reason for this behavior is evident.

Predicted versus actual fatigue lives for the three methods employed are presented in Fig. 11. In general, plastic work interaction yields conservative life predictions, $\Delta J$ crack growth estimates are slightly nonconservative, and conventional linear damage predictions are highly nonconservative.

## 5. CONCLUSIONS

(1) Using conventional methods of fatigue analysis, one will calculate nonconservative fatigue life predictions for histories containing numerous subcycles and only a few large amplitude cycles.

(2) The degree of nonconservatism observed in this study is greater for histories having:

   (a) .005 strain amplitude major cycles rather than for those in which the strain amplitude of major cycles is .010

   (b) greater numbers of subcycles per block (up to $10^4$ cycles in this investigation)

   (c) .001 subcycle strain amplitude rather than for those in which the subcycle strain amplitude is .002

(3) The difference between the outer envelope of the block and the plain cycle hysteresis loop in the varying mean stress test does not account for the reduction in fatigue life.

(4) The existence of mean stresses also does not explain the difference in fatigue life in the varying mean stress histories.

(5) There may be a "minimum damage" level that must be exceeded before subcycles cause significant damage. Once this level is exceeded, the subcycles may cause a high percentage of the damage. Both segments of the life, before and after the "minimum" is reached, must be taken into account in proposing fatigue life prediction models.

(6) Identification of an event for damage assessment needs to be redefined.

(7) Harder materials may display increased memory effects (i.e. sensitivity to initial or periodic overstrains) but be less sensitive to subcycles hung within a block (i.e. interactive effects).

(8) More conservative fatigue life predictions are achieved with plastic work interaction, and $\Delta J$ crack growth, than with conventional linear damage.

(9) Plastic work interaction generally predicts conservative fatigue lives whereas $\Delta J$ crack growth estimates are slightly nonconservative.

(10) Both plastic work interaction and $\Delta J$ crack growth analyses employ the summation of the product of a stress-strain quantity raised to a power to achieve an interactive relation between major cycle and subcycle.

## REFERENCES


1. Paris, P. C., "The Fracture Mechanics Approach to Fatigue," Proceedings of the Tenth Sagamore Conference, Syracuse University Press, 1963.

2. Forman, R. G., Kearney, V. E. and Engle, R. M., "Numerical Analysis of Crack Propagation in Cyclic-Loaded Structures," Journal of Basic Engineering, Transactions ASME, Vol. 89, Series D, September, pp. 459-464, 1967.

3. Peterson, R. E., "Analytic Approach to Stress Concentration Effect in Fatigue of Aircraft Materials," Proceedings of the Symposium on Fatigue of Aircraft Structures, 1959 WADC Technical Report, pp. 59-507, August, 1959.

4. Neuber, H., "Theory of Notch Stresses," Principles for Exact Stress Calculations, J. W. Edwards, Ann Arbor, Michigan, 1946.

5. Topper, T. H., Wetzel, R. M. and Morrow, J., "Neuber's Rule Applied to Fatigue of Notched Specimens," Journal of Materials, Vol. 4, No. 1, pp. 200-209, 1969.

6. Neuber, H., "Theory of Stress Concentration for Shear Strained Prismatic Bodies with Arbitrary Nonlinear Stress-Strain Law," Journal of Applied Mechanics, Transactions ASME, Vol. 28, No. 4, pp. 544-560, 1961.

7. Socie, D. F., "Fatigue Life Estimates for Bluntly Notched Members," Journal of Engineering Materials and Technology, Transactions ASME, Vol. 102, pp. 153-158, 1980.

8. Kurath, P., Socie, D. F. and Morrow, J., "A Nonarbitrary Fatigue Crack Size Concept to Predict Total Fatigue Lives," Technical Report AFDL-TR-79-3144, Air Force Flight Dynamics Laboratory, Wright-Patterson AFB, Ohio, December, 1979.

9. Dowling, N. E., "Notched Member Fatigue Life Predictions Combining Crack Initiation and Propagation," Fatigue of Engineering Materials and Structures, Vol. 2, No. 2, pp. 129-138, 1979.

10. Dowling, N. E., "Fatigue Failure Predictions for Complicated Stress-Strain Histories," Journal of Materials, Vol. 7, No. 1, pp. 71-87, March, 1972.

11. Socie, D. F. and Kurath, P., "Cycle Counting for Variable Amplitude Crack Growth," Fracture Control Program Report No. 37, University of Illinois, College of Engineering, Urbana, Illinois, 1981.

12. Downing, S. D. and Socie, D. F., "Simple Rainflow Counting Algorithms," International Journal of Fatigue, Vol. 4, No. 1, 1982

13. Miner, M. A., "Cumulative Damage in Fatigue," Journal of Applied Mechanics, Transactions ASME, Vol. 12, pp. A159-A164, September, 1945.

14. Leve, H. L., "Cumulative Damage Theories," Metal Fatigue: Theory and Design, A. F. Madayag, Ed., John Wiley and Sons, Inc., pp. 171-203, 1969.

15. Brose, W. R., Dowling, N. E. and Morrow, JoDean, "Effect of Periodic Large Strain Cycles on the Fatigue Behavior of Steels," SAE Paper 740221, Society of Automotive Engineers, 11 pp, 1974.

16. Haibach, E. and Schütz, D., "Fatigue Life Evaluation with Particular Attention to Local Strain and Stress Time Histories," presented at the Conference on Designing Against Fatigue-Implications of Recent Findings on Complex Situations, Institution of Mechanical Engineers, Applied Mechanics Group, London, October 9, 1974.

17. Dowling, N. E., "Fatigue Life and Inelastic Strain Response Under Complex Histories for an Alloy Steel," Journal of Testing and Evaluation, Vol. 1, No. 4, pp. 271-287, July, 1973.

18. Socie, D. F. and Artwohl, P. J., "Effect of Spectrum Editing on Fatigue Crack Initiation and Propagation in a Notched Member," Fracture Control Program Report No. 31, University of Illinois, College of Engineering, Urbana, Illinois, 17 pp, December, 1978.

19. Conle, F. A., "An Examination of Variable Amplitude Histories in Fatigue," Ph.D. Thesis, University of Waterloo, Waterloo, Ontario, Canada, 1979.

20. Teledyne CAE, "Structural Life Prediction/Correlation Program, Task II - Engine Component Analysis," Technical Report AFAPL-TR-79-2082, Air Force Aero-Propulsion Laboratory, Wright-Patterson AFB, Ohio, 66 pp, August, 1979.

21. Manson, S. S. and Halford, G. R., "Practical Implementation of the Double Linear Damage Rule and Damage Curve Approach for Treating Cumulative Fatigue Damage," NASA Technical Memorandum 81517, NASA Lewis Research Center, Cleveland, Ohio, 49 pp, April, 1980.

22. Hunter, M. S. and Fricke, W. G., Jr., "Fatigue Crack Propagation in Aluminum Alloys," Proceedings of the American Society for Testing Materials, Vol. 56, 1956.

23. Dowling, N. E., "Crack Growth During Low-Cycle Fatigue of Smooth Axial Specimens," Cyclic Stress-Strain and Plastic Deformation Aspects of Fatigue Crack Growth, ASTM STP 637, American Society for Testing and Materials, pp. 97-121, 1977.

24. Nisitani, H. and Takao, K., "Behavior of a Tip of a Non-propagating Fatigue Crack During One Stress Cycle," Engineering Fracture Mechanics, Vol. 6, pp. 253-260, 1974.

25. Nisitani, H. and Takao, K., "Fatigue Crack Acceleration and Closure in Rotating Bending Tests of 0.54% Carbon Steel," Engineering Fracture Mechanics, Vol. 10, pp. 855-866, 1978.

26. Frost, N. E., "Notch Effects and the Critical Alternating Stress Required to Propagate a Crack in an Aluminum Alloy Subject to Fatigue Loading," Journal of Mechanical Engineering Science, Vol. 2, No. 2, pp. 109-119, 1960.

27. El Haddad, M. H., Smith, K. N. and Topper, T. H., "Fatigue Crack Propagation of Short Cracks," Journal of Engineering Materials and Technology, Transactions ASME, Vol. 101, No. 1, pp. 42-46, 1979.

28. Masing, G., "Eigenspannungen and Verfestigung Bein Messing," Proceedings of the Second International Congress of Applied Mechanics, Zurich, 1926.

29. Watson, P., Hoddinott, D. S. and Norman, J. P., "Periodic Overloads and Random Fatigue Behavior," Cyclic Stress-Strain Behavior--Analysis, Experimentation, and Prediction, ASTM STP 519, American Society for Testing and Materials, pp. 271-284, 1973.

30. Corten, H. T. and Dolan, T. J., "Cumulative Fatigue Damage," Proceedings of the International Conference on Fatigue of Metals, London, Institution of Mechanical Engineers and American Society of Mechanical Engineers, pp. 235-246, 1956.

31. Ewing, J. A. and Humfrey, J. C. W., "The Fracture of Metals Under Repeated Alternations of Stress," Philosophical Transactions of the Royal Society of London, Series A, Vol. 200, p. 241, 1903.

32. Morrow, J., "Cyclic Plastic Strain Energy and Fatigue of Metals," Internal Friction, Damping and Cycle Plasticity, ASTM STP 378, American Society for Testing and Materials, pp. 45-87, 1964.

33. Halford, G. R., "The Energy Required for Fatigue," Journal of Materials, Vol. 1, No. 1, pp. 3-18, 1966.

34. Morrow, J., "Fatigue Properties of Metals," unpublished manuscript, 1964.

35. Srawley, J. E. and Brown, W. F., "Fracture Toughness Testing Methods," ASTM STP 381, American Society for Testing and Materials, pp. 133-145, 1965.

36. Paris, P. C., Gomez, M. P. and Anderson, W. E., "A Rational Analytic Theory of Fatigue," The Trend in Engineering, University of Washington, pp. 9-14, 1961.

37. Rice, J. R., "Path Independent Integral and the Approximate Analysis of Strain Concentration by Notches and Cracks," Journal of Applied Mechanics, Vol. 35, Transactions ASME, pp. 379-386, June, 1968.

38. Begley, J. A. and Landes, J. D., "The J Integral as a Fracture Criterion," Fracture Toughness, Proceedings of the 1971 National Symposium on Fracture Mechanics, Part II, ASTM STP 514, American Society for Testing and Materials, pp. 1-20, 1972.

39. Dowling, N. E. and Begley, J. A., "Fatigue Crack Growth During Gross Plasticity and the J-integral," Westinghouse Research Labs., Scientific Paper 74-1E7-CREEP-P1, 1974. Also in ASTM STP 590, American Society for Testing and Materials, pp. 82-103, 1976.

40. Kaisand, L. R. and Mowbray, D. F., "Relationships Between Low-Cycle Fatigue and Fatigue Crack Growth Rate Properties," Journal of Testing and Evaluation, Vol. 7, No. 5, pp. 270-280, 1979.

41. Mowbray, D. F., "Derivation of a Low-Cycle Fatigue Relationship Employing the J-integral Approach to Crack Growth," ASTM STP 601, American Society for Testing and Materials, pp. 33-46, 1976.

42. El Haddad, M. H., Dowling, N. E., Topper, T. H. and Smith, K. N., "J-integral Applications for Short Fatigue Cracks at Notches," International Journal of Fracture, Vol. 16, No. 1, pp. 15-30, 1980.

43. Sehitoglu, H., "Fatigue Life Prediction of Notched Members Based on Local Strain and Elastic-Plastic Fracture Mechanics Concepts," to be published in Engineering Fracture Mechanics, 1982.

44. Irwin, G. R., "The Crack Extension Force for a Part-Through Crack in a Plate," Journal of Applied Mechanics, Transactions ASME, pp. 651-654, 1962.

45. Shih, C. F. and Hutchinson, J. W., "Fully Plastic Solutions and Large Scale Yielding Estimates for Planes Stress Crack Problems, Report No. DEAP-S-14, Division of Engineering and Applied Physics, Harvard University, Cambridge, Massachusetts, July, 1975. Also in Journal of Engineering Materials and Technology, Transactions ASME, pp. 289-295, 1976.

46. Socie, D. F., Mitchell, M. R. and Caulfield, E. M., "Fundamentals of Modern Fatigue Analysis," Fracture Control Program Report No. 26, University of Illinois, College of Engineering, Urbana, Illinois, April, 1977.

47. Hertzberg, R. W., Deformation and Fracture Mechanics of Engineering Materials, John Wiley and Sons, 1976.

48. Fash, J. W., "Fatigue Crack Initiation and Growth in Gray Cast Iron," Fracture Control Program Report No. 35, University of Illinois, College of Engineering, Urbana, Illinois, October, 1980.

49. Raske, D. T. and Morrow, JoDean, "Mechanics of Materials in Low Cycle Fatigue Testing," Manual on Low Cycle Fatigue Testing, ASTM STP 465, American Society for Testing and Materials, pp. 1-26, 1969.

50. Grover, H. J., "An Observation Concerning the Cycle Ratio in Cumulative Damage," Fatigue of Aircraft Structures, ASTM STP 274, American Society for Testing and Materials, pp. 120-124, 1960.

51. Morrow, JoDean, "Fatigue Properties in Metals," Fatigue Design Handbook, Advances in Engineering, Vol. 4, J. A. Graham, Ed., Society of Automotive Engineers, Inc., pp. 21-29, 1968.

52. Dieter, G. E., Jr. Mechanical Metallurgy, McGraw-Hill, 2nd Edition, pp. 344-346, 1976.

# APPENDIX

## MEAN STRESS-STRAIN LIFE COEFFICIENTS

Life predictions for all histories that involved subcycles applied at a non-zero mean stress were made using the well known Morrow mean stress parameter (51):

$$\frac{\Delta\sigma}{2} = (\sigma_f' - \sigma_o)(2N_f)^b$$

The derivation of a strain-life equation using this parameter from Ref. 51 is presented below.

The strain-life relationship for cases which do not involve mean stresses is

$$\frac{\Delta\varepsilon}{2} = \frac{\sigma_f'}{E}(2N_f)^b + \varepsilon_f'(2N_f)^c. \qquad \text{[A-1]}$$

The position of a subcycle hysteresis loop within a major loop does not significantly change the size or shape of the subcycle loop (the subcycle loop size and shape is not dependent on mean stress). Therefore, as mean stress changes, $\Delta\varepsilon_p$ and $\Delta\varepsilon_e$ must remain the same.

If

$$\frac{\Delta\varepsilon_e}{2} = \frac{\sigma_f'}{E}(2N_f)^b = \frac{\sigma_f' - \sigma_o}{E}(2N_{fo})^b, \qquad \text{[A-2]}$$

then

$$\frac{\Delta\varepsilon_p}{2} = \varepsilon_f'(2N_f)^c = \varepsilon_{fo}'(2N_{fo})^c, \qquad \text{[A-3]}$$

or

$$\frac{\Delta\varepsilon}{2} = \left(\frac{\sigma_f' - \sigma_o}{E}\right)(2N_{fo})^b + \varepsilon_{fo}'(2N_{fo})^c. \qquad \text{[A-4]}$$

Rearranging Eq. A-2, we obtain

$$\frac{2N_{fo}}{2N_f} = \left(\frac{\sigma_f'}{\sigma_f - \sigma_o}\right)^{1/b}, \qquad \text{[A-5]}$$

and rearranging Eq. A-3, we obtain

$$\varepsilon'_{fo} = \varepsilon'_f \left( \frac{2N_f}{2N_{fo}} \right)^c . \qquad \text{[A-6]}$$

Combining Eqs. A-5 and A-6 produces

$$\varepsilon'_{fo} = \varepsilon'_f \left( \frac{\sigma'_f - \sigma_o}{\sigma'_f} \right)^{c/b} , \qquad \text{[A-7]}$$

therefore, $$\frac{\Delta\varepsilon}{2} = \frac{\sigma'_f - \sigma_o}{E} (2N_{fo})^b + \varepsilon'_f \left( \frac{\sigma'_f - \sigma_o}{\sigma'_f} \right)^{c/b} (2N_{fo})^c . \qquad \text{[A-8]}$$

TABLE 1

MATERIAL PROPERTIES

Designation: ASTM A-36 Hot Rolled Strip

Chemistry (w/o): (Average of several tests)

| C | Mn | P | S | Si | Ni | Cr | Mo | Cu | B | V |
|---|---|---|---|---|---|---|---|---|---|---|
| .25 | .83 | .01 | .025 | .255 | .10 | .09 | .01 | .016 | --- | --- |

Hardness: 140 BHN (80 $R_b$)

Monotonic Properties: (Average of two tests)

| | |
|---|---|
| Modulus of Elasticity, E | 210,000 MPa |
| Yield Strength, .2% $S_y$ | 351 MPa |
| Ultimate Strength, $S_u$ | 540 MPa |
| Reduction in Area, %RA | 66.8% |
| True Fracture Strength, $\sigma_f$ | 1,173 MPa<br>1,092 MPa* |
| True Fracture Ductility, $\varepsilon_f$ | 1.10 |
| Strain Hardening Exponent, n | .236 |
| Strength Coefficient, K | 992 MPa |

*Corrected for necking as proposed by Bridgman (52).

TABLE 2

CYCLIC PROPERTIES

| | |
|---|---|
| **From Constant Amplitude Strain Controlled Tests:** | |
| Modulus of Elasticity, E | 200,000 MPa |
| Yield Strength, .2% $S_y$ | 330 MPa |
| Strain Hardening Exponent, n' | .226 |
| Strength Coefficient, K' | 1,336 MPa |
| Fatigue Strength Coefficient, $\sigma'_f$ | 1,118 MPa |
| Fatigue Ductility Coefficient, $\varepsilon'_f$ | .338 |
| Fatigue Strength Exponent, b | -.110 |
| Fatigue Ductility Exponent, c | -.480 |
| Transition Fatigue Life, $2N_t$ | 90,000 rev |
| **From Overstrain Tests:** | |
| Fatigue Strength Coefficient, $\sigma'_f$ | 1,054 MPa |
| Fatigue Ductility Coefficient, $\varepsilon'_f$ | .487 |
| Fatigue Strength Exponent, b | -.105 |
| Fatigue Ductility Exponent, c | -.521 |
| **Plastic Work Coefficients:** | |
| Plastic Work Coefficient, D' | 2,690 |
| Plastic Work Exponent, d | -.21 |
| **ΔJ Crack Growth Coefficients:** | |
| Crack Growth Coefficient, C | $1.97 \times 10^{-5}$ |
| Crack Growth Exponent, m | 1.78 |

TABLE 3

CONSTANT AMPLITUDE STRAIN CONTROLLED TESTS
(RAMP WAVEFORM)

| Specimen No. | $\Delta\varepsilon/2$ | $2N_f$ | $\overline{\Delta\sigma}/2$ (MPa) | $\overline{\Delta\varepsilon_p}/2$ |
|---|---|---|---|---|
| 92 | .00100 | $>10^6$ | 206 | <.00001 |
| 48 | .00180 | $>10^6$ | 258 | .00053 |
| 26 | .00202 | 359,700 | 261 | .00079 |
| 84 | .00202 | 416,700 | 261 | .00074 |
| 35A* | .00306 | 56,000 | 305 | .00155 |
| 35 | .00306 | 65,650 | 305 | .00158 |
| 36 | .00410 | 25,220 | 340 | .00239 |
| 36A* | .00420 | 27,160 | 343 | .00245 |
| 38 | .00510 | 15,890 | 372 | .00323 |
| 76 | .00509 | 11,870 | 363 | .00324 |
| 80 | .00510 | 15,950 | 369 | .00322 |
| 38A* | .00520 | 16,120 | 378 | .00335 |
| 39 | .00756 | 5,119 | 404 | .00554 |
| 39A* | .00770 | 4,475 | 417 | .00565 |
| 41A | .0102 | 2,671 | 438 | .00783 |
| 82 | .0102 | 2,952 | 440 | .00784 |
| 40* | .0103 | 2,981 | 450 | .00794 |
| 94 | .0131 | 1,175 | 440 | .01070 |
| 97 | .0132 | 1,725 | 432 | .01070 |
| 96 | .0151 | 989 | 444 | .0125 |

*Denotes replicated sample

TABLE 4

SMALL CRACK MEASUREMENTS FROM CONSTANT AMPLITUDE SMOOTH SPECIMEN REPLICAS

| Specimen No. | Crack Length a (mm) | Reversals 2N |
|---|---|---|
| 35A | .075 | 8,216 |
| | .080 | 16,220 |
| | .103 | 24,220 |
| | .245 | 32,220 |
| | .491 | 40,220 |
| 36A | .084 | 11,650 |
| | .125 | 14,410 |
| | .151 | 16,450 |
| | .356 | 18,848 |
| | .582 | 21,250 |
| | 1.10 | 23,650 |
| | 2.53 | 26,050 |
| 38A | .028 | 8,448 |
| | .084 | 10,050 |
| | .245 | 13,250 |
| | 2.47 | 14,850 |
| 39A | .081 | 2,012 |
| | .089 | 2,512 |
| | .134 | 3,012 |
| | .201 | 3,512 |
| | .220 | 4,012 |
| 40 | .089 | 976 |
| | .134 | 1,216 |
| | .178 | 1,456 |
| | .223 | 1,696 |
| | .356 | 2,176 |

TABLE 5

STRAIN CONTROLLED OVERSTRAIN TESTS

| Specimen No. | Type | $\Delta\varepsilon/2$ | $2N_f$ | $\overline{\Delta\sigma}/2$ | $\overline{\Delta\varepsilon_p}/2$ |
|---|---|---|---|---|---|
| 34A | I | .00150 | $>3.5 \times 10^6$ | 249 | .00030 |
| 47 | P | .00150 | 2,634,000 | 248 | .00029 |
| 49 | I | .00180 | 474,700 | 255 | .00057 |
| 50 | P | .00180 | 576,700 | 252 | .00058 |
| 44 | I | .00202 | 206,400 | 258 | .00079 |
| 45 | I | .00306 | 49,830 | 293 | .00159 |
| 43 | I | .00410 | 21,990 | 331 | .00242 |
| 46 | I | .00508 | 15,520 | 368 | .00322 |

Type abbreviations: I = Initial overstrain

P = Periodic overstrain

TABLE 6

VARIABLE MEAN STRESS SUBCYCLE TEST RESULTS

| Specimen No. | No. of Subcycles Per Block | Major Cycle | | | Subcycle | | | Life (Blocks) |
|---|---|---|---|---|---|---|---|---|
| | | $\Delta\varepsilon/2$ | $\Delta\varepsilon_p/2$ | $\Delta\sigma/2$ (MPa) | $\Delta\varepsilon/2$ | $\Delta\varepsilon_p/2$ | $\Delta\sigma/2$ (MPa) | |
| 54 | 20 | .005 | .0034 | 339 | .001 | .0001 | 183 | 5,350 |
| 70 | 40 | .005 | .0036 | 333 | .002 | .0008 | 268 | 1,079 |
| 74 | 100 | .005 | .0035 | 314 | .002 | .0008 | 259 | 530 |
| 53 | 20 | .010 | .0081 | 421 | .001 | .0001 | 183 | 1,010 |
| 59 | 40 | .010 | .0081 | 420 | .001 | .0001 | 184 | 698 |
| 58 | 100 | .010 | .0082 | 424 | .001 | NA* | 184 | 860 |
| 65 | 40 | .010 | .0083 | 392 | .002 | .0007 | 279 | 581 |
| 64 | 100 | .010 | .0083 | 390 | .002 | .0007 | 280 | 281 |

*Not Available

TABLE 7

INTERSPERSED VARYING MEAN STRESS SUBCYCLE TEST RESULTS

| Specimen No. | Block (B) or Loop (C) | Limit Block/Loop Sequence | No. of Subcycles Block | Major Cycle $\Delta\varepsilon/2$ | Major Cycle $\overline{\Delta\varepsilon_p}/2$ | Major Cycle $\overline{\Delta\sigma}/2$ (MPa) | Subcycle $\Delta\varepsilon/2$ | Subcycle $\overline{\Delta\varepsilon_p}/2$ | Subcycle $\overline{\Delta\sigma}/2$ (MPa) | Total Life |
|---|---|---|---|---|---|---|---|---|---|---|
| 52 | B | 500 | 20 | .005 | .0033 | 352 | .001 | .0001 | 179 | 3,111 (B) |
| | C | 500 | | .005 | NA * | 364 | | | | 2,734 (C) |
| 72 | B | 500 | 40 | .005 | NA | NA | .002 | NA | NA | 1,046 (B) |
| | C | 500 | | .005 | .0033 | 358 | | | | 611 (C) |
| 69 | B | 50 | 100 | .005 | .0035 | 332 | .002 | .0008 | 263 | 501 (B) |
| | C | 50 | | .005 | .0032 | 351 | | | | 472 (C) |
| 73 | B | 50 | 100 | .005 | .0035 | 317 | .002 | .0008 | 261 | 561 (B) |
| | C | 50 | | .005 | .0033 | 339 | | | | 563 (C) |
| 51 | B | 100 | 20 | .010 | .0079 | 424 | .001 | .0001 | 174 | 613 (B) |
| | C | 100 | | .010 | NA | 436 | | | | 611 (C) |
| 56 | B | 100 | 40 | .010 | .0084 | 415 | .001 | .0001 | 184 | 435 (B) |
| | C | 100 | | .010 | NA | 426 | | | | 411 (C) |
| 60 | B | 100 | 40 | .010 | .0082 | 431 | .001 | .0001 | 189 | 342 (B) |
| | C | 100 | | .010 | NA | 440 | | | | 311 (C) |
| 57 | B | 50 | 100 | .010 | .0081 | 414 | .001 | .0001 | 184 | 510 (B) |
| | C | 50 | | .010 | NA | 425 | | | | 485 (C) |
| 63 | B | 50 | 40 | .010 | .0082 | 396 | .002 | .0007 | 277 | 399 (B) |
| | C | 50 | | .010 | .0080 | 420 | | | | 361 (C) |
| 62 | B | 50 | 100 | .010 | .0083 | 367 | .002 | .0007 | 265 | 361 (B) |
| | C | 50 | | .010 | .0080 | 412 | | | | 311 (C) |

*Not Available

TABLE 8

ZERO MEAN STRESS SUBCYCLE TEST RESULTS

| Specimen No. | No. of Subcycles Per Block | Major Cycle | | | Subcycle | | | Life (Blocks) |
|---|---|---|---|---|---|---|---|---|
| | | $\Delta\varepsilon/2$ | $\Delta\varepsilon_p/2$ | $\Delta\sigma/2$ (MPa) | $\Delta\varepsilon/2$ | $\Delta\varepsilon_p/2$ | $\Delta\sigma/2$ (MPa) | |
| 78* | $10^2$ | .005 | .0032 | 371 | .001 | .00009 | 187 | 4,688 |
| 81 | $10^2$ | .005 | .0032 | 370 | .001 | .00010 | 186 | 4,368 |
| 90 | $10^3$ | .005 | .0032 | 345 | .001 | .00008 | 180 | 624 |
| 91 | $10^3$ | .005 | .0032 | 345 | .001 | .00008 | 180 | 683 |
| 92 | $10^4$ | .005 | .0032 | 337 | .001 | .00008 | 181 | 293 |
| 75 | $10^2$ | .005 | .0033 | 336 | .002 | .00070 | 260 | 648 |
| 79 | $10^2$ | .01 | .0079 | 456 | .001 | .00009 | 187 | 1,180 |
| 87 | $10^3$ | .01 | .0077 | 428 | .001 | .00007 | 185 | 458 |
| 77 | $10^2$ | .01 | .0080 | 420 | .002 | .00065 | 283 | 344 |

*Mean strain was compressive (subcycle on loading part of loop).

TABLE 9

MAXIMUM-MEAN STRESS AND MINIMUM-MEAN STRESS SUBCYCLE TEST RESULTS

| Specimen No. | No. of Subcycles Per Block | Major Cycle | | | Subcycle | | | (Blocks) |
|---|---|---|---|---|---|---|---|---|
| | | $\Delta\varepsilon/2$ | $\Delta\varepsilon_p/2$ | $\Delta\sigma/2$ (MPa) | $\Delta\varepsilon/2$ | $\Delta\varepsilon_p/2$ | $\Delta\sigma/2$ (MPa) | |
| 95 | $10^3$ | .005 | .00335 | 328 | .001 | .00010 | 165 | <1,320 |
| 88 | $10^3$ | .005 | .00332 | 338 | .001 | .00010 | 172 | 1,386 |
| 67 | $10^3$ | .01 | .00795 | 429 | .001 | .00010 | 178 | 472 |
| 68* | $10^3$ | .01 | .00787 | 444 | .001 | .00008 | 183 | ≈1,100 |

All mean stresses tensile except as noted.

*Mean stress was compressive (subcycle on compressive loop tip).

TABLE 10

EDITED VARYING MEAN STRESS TEST RESULTS

| Specimen No. | No. of Subcycles Per Block | No. of Initial Plain Cycles | Block Loop (B) or Plain Cycle (C) | Major Cycle ($\frac{\Delta\varepsilon}{2}$ = .005) | | Subcycle ($\frac{\Delta\varepsilon}{2}$ = .001) | | Blocks to Failure after Initial Plain Cycles |
|---|---|---|---|---|---|---|---|---|
| | | | | $\Delta\varepsilon_p/2$ | $\Delta\sigma/2$ (MPa) | $\Delta\varepsilon_p/2$ | $\Delta\sigma/2$ (MPa) | |
| 100 | $10^2$ | 512 | B | .00320 | 347 | .00008 | 178 | 2,043 |
| | | | C | .00325 | 335 | --- | --- | |
| 86 | $10^2$ | 1,024 | B | .0032 | 356 | .00010 | 184 | 2,023 |
| | | | C | .0033 | NA* | --- | --- | |
| 99 | $10^2$ | 2,048 | B | .00322 | 348 | .00009 | 174 | 1,955 |
| | | | C | .00330 | 330 | --- | --- | |

*Not Available

TABLE 11

VARIABLE MEAN STRESS SUBCYCLE PREDICTIONS

| Amplitude Cyc/Subcyc | No. of Subcycles Per Block | Actual Life (Blocks) | Plastic Work Interaction (Blocks) | Crack Growth (Blocks) | Linear* Damage (Blocks) |
|---|---|---|---|---|---|
| .005/.001 | 1,000 | | 295 | 559 | 4,473 |
| | 100 | | 2,269 | 3,562 | 8,043 |
| | 40 | | 4,094 | 5,547 | 8,217 |
| | 20 | 5,350 | 5,594 | 6,812 | 8,217 |
| .005/.002 | 1,000 | | 45 | 58 | 214 |
| | 100 | 530 | 431 | 550 | 1,759 |
| | 40 | 1,079 | 1,005 | 1,258 | 3,386 |
| | 20 | | 1,804 | 2,203 | 4,894 |
| .01/.001 | 1,000 | | 110 | 401 | 1,165 |
| | 100 | 860 | 632 | 1,084 | 1,318 |
| | 40 | 698 | 924 | 1,223 | 1,329 |
| | 20 | 1,010 | 1,093 | 1,277 | 1,333 |
| .01/.002 | 1,000 | | 18 | 54 | 189 |
| | 100 | 281 | 157 | 397 | 831 |
| | 40 | 581 | 334 | 686 | 1,075 |
| | 20 | | 534 | 907 | 1,192 |

*With no mean stress effects

TABLE 12

INTERSPERSED VARIABLE MEAN STRESS SUBCYCLE PREDICTIONS

| Amplitude Cyc/Subcyc | No. of Subcycles Per Block | Limit Blk/Loop Sequence | Actual Life (Blk/Cyc) | Plastic Work Interaction (Blk/Cyc) | Crack Growth (Blk/Cyc) | Linear* Damage (Blk/Cyc) |
|---|---|---|---|---|---|---|
| .005/.001 | 1,000 | 50 | | 286/263 | 526/513 | 2,972/2,963 |
| | | 100 | | 287/227 | 427/510 | 2,990/2,927 |
| | | 500 | | 287/255 | 526/511 | 3,011/2,885 |
| | 100 | 50 | | 1,813/1,775 | 2,547/2,513 | 4,213/4,203 |
| | | 100 | | 1,825/1,727 | 2,542/2,527 | 4,227/4,188 |
| | | 500 | | 1,881/1,511 | 2,548/2,511 | 4,389/4,011 |
| | 40 | 50 | | 2,813/2,763 | 3,363/3,396 | 4,345/4,313 |
| | | 100 | | 2,827/2,732 | 3,647/3,023 | 4,331/4,327 |
| | | 500 | | 2,930/2,511 | 3,011/3,240 | 4,511/4,140 |
| | 20 | 50 | | 3,431/3,413 | 3,813/3,821 | 4,379/4,363 |
| | | 100 | | 3,427/3,419 | 3,859/3,827 | 4,413/4,327 |
| | | 500 | 3,111/2,734 | 3,511/3,287 | 3,511/3,630 | 4,511/4,228 |
| .005/.002 | 1,000 | 50 | | 45/31 | 43/32 | 210/163 |
| | 100 | 50 | 501/472<br>561/563 | 413/375 | 518/513 | 1,467/1,463 |
| | | 100 | | 415/327 | 524/547 | 1,475/1,427 |
| | | 500 | | 419/255 | 518/511 | 1,511/1,245 |
| | 40 | 50 | | 906/863 | 1,107/1,063 | 2,460/2,413 |
| | | 100 | | 911/827 | 1,112/1,027 | 2,455/2,427 |
| | | 500 | 1,046/611 | 946/511 | 1,114/1,011 | 2,511/2,280 |
| | 20 | 50 | | 1,505/1,463 | 1,763/1,763 | 3,163/3,122 |
| | | 100 | | 1,512/1,427 | 1,772/1,727 | 3,160/3,127 |
| | | 500 | | 1,511/1,434 | 1,826/1,511 | 3,225/3,011 |

*With no mean stress effects

TABLE 13

INTERSPERSED VARIABLE MEAN STRESS SUBCYCLE PREDICTIONS

| Amplitude Cyc/Subcyc | No. of Subcycles Per Block | Limit Blk/Loop Sequence | Actual Life (Blk/Cyc) | Plastic Work Interaction (Blk/Cyc) | Crack Growth (Blk/Cyc) | Linear* Damage (Blk/Cyc) |
|---|---|---|---|---|---|---|
| .01/.001 | 1,000 | 50 | | 105/63 | 263/295 | 631/613 |
| | 100 | 50 | 510/485 | 437/413 | 563/581 | 664/663 |
| | | 100 | | 430/427 | 527/564 | 699/627 |
| | | 500 | | 511/256 | 670/511 | 814/511 |
| | 40 | 50 | | 563/523 | 662/613 | 670/663 |
| | | 100 | 435/411 | 566/527 | 649/627 | 706/627 |
| | | | 342/311 | | | |
| | | 500 | | 571/511 | 755/511 | 821/511 |
| | 20 | 50 | | 613/587 | 613/643 | 672/663 |
| | | 100 | 613/611 | 627/570 | 678/627 | 708/627 |
| | | 500 | | 675/511 | 789/511 | 824/511 |
| .01/.002 | 1,000 | 50 | | 17/15 | 37/32 | 166/163 |
| | 100 | 50 | | 144/113 | 263/283 | 513/511 |
| | | 100 | 361/311 | 142/127 | 227/236 | 527/489 |
| | | 500 | | 142/127 | 227/236 | 513/511 |
| | 40 | 50 | 399/361 | 268/263 | 413/435 | 613/576 |
| | | 100 | | 277/227 | 467/427 | 627/557 |
| | | 500 | | 270/255 | 256/215 | 664/511 |
| | 20 | 50 | | 389/363 | 559/513 | 645/613 |
| | | 100 | | 404/327 | 549/527 | 633/627 |
| | | 500 | | 432/255 | 560/511 | 736/511 |

*With no mean stress effects

TABLE 14

ZERO MEAN STRESS SUBCYCLE PREDICTIONS

| Amplitude Cyc/Subcyc | No. of Subcycles Per Block | Actual Life (Blocks) | Plastic Work Interaction (Blocks) | Crack Growth (Blocks) | Linear Damage (Blocks) |
|---|---|---|---|---|---|
| .005/.001 | 1,000 | 624<br>683 | 295 | 1,889 | 4,473 |
| | 100 | 4,688<br>4,368 | 2,269 | 6,457 | 8,043 |
| | 40 | | 4,094 | 7,696 | 8,217 |
| | 20 | | 5,594 | 8,217 | 8,217 |
| .005/.002 | 1,000 | | 45 | 156 | 214 |
| | 100 | 648 | 431 | 1,350 | 1,759 |
| | 40 | | 1,005 | 2,746 | 3,386 |
| | 20 | | 1,804 | 4,189 | 4,894 |
| .01/.001 | 1,000 | 458 | 110 | 847 | 1,165 |
| | 100 | 1,180 | 632 | 1,264 | 1,318 |
| | 40 | | 924 | 1,306 | 1,329 |
| | 20 | | 1,093 | 1,321 | 1,333 |
| .01/.002 | 1,000 | | 18 | 137 | 189 |
| | 100 | 344 | 157 | 714 | 831 |
| | 40 | | 334 | 991 | 1,075 |
| | 20 | | 534 | 1,138 | 1,192 |

TABLE 15

EDITED VARIABLE MEAN STRESS SUBCYCLE PREDICTIONS

| Amplitude Cyc/Subcyc | No. of Subcycles | No. of Initial Plain Cycles | Actual Life (Blocks) | Plastic Work Interaction (Blocks) | Crack Growth (Blocks) | Linear* Damage (Blocks) |
|---|---|---|---|---|---|---|
| .005/.001 | 100 | 512 | 2,043 | 2,138 | 3,521 | 7,577 |
| | | 1,024 | 2,023 | 2,006 | 3,148 | 7,111 |
| | | 2,048 | 1,955 | 1,742 | 2,735 | 6,178 |
| | 40 | 512 | | 3,856 | 5,225 | 8,003 |
| | | 1,024 | | 3,619 | 4,903 | 7,510 |
| | | 2,048 | | 3,144 | 4,260 | 6,525 |
| | 20 | 512 | | 5,269 | 6,417 | 8,156 |
| | | 1,024 | | 4,945 | 6,022 | 7,653 |
| | | 2,048 | | 4,296 | 5,232 | 6,649 |
| .005/.002 | 100 | 512 | | 406 | 518 | 1,656 |
| | | 1,024 | | 381 | 486 | 1,555 |
| | | 2,048 | | 331 | 422 | 1,351 |
| | 40 | 512 | | 946 | 1,185 | 3,189 |
| | | 1,024 | | 888 | 1,112 | 2,993 |
| | | 2,048 | | 772 | 966 | 2,600 |
| | 20 | 512 | | 1,699 | 2,075 | 4,610 |
| | | 1,024 | | 1,594 | 1,947 | 4,326 |
| | | 2,048 | | 1,385 | 1,692 | 3,758 |
| .01/.001 | 100 | 256 | | 1,081 | 876 | 1,065 |
| | | 512 | | 390 | 669 | 813 |
| | | 1,024 | | 148 | 254 | 308 |
| | 40 | 256 | | 747 | 989 | 1,074 |
| | | 512 | | 570 | 754 | 820 |
| | | 1,024 | | 216 | 286 | 311 |
| | 20 | 256 | | 883 | 1,033 | 1,078 |
| | | 512 | | 674 | 788 | 823 |
| | | 1,024 | | 256 | 299 | 312 |
| .01/.002 | 100 | 256 | | 127 | 321 | 672 |
| | | 512 | | 97 | 245 | 512 |
| | | 1,024 | | 37 | 93 | 195 |
| | 40 | 256 | | 270 | 555 | 869 |
| | | 512 | | 206 | 423 | 663 |
| | | 1,024 | | 78 | 160 | 252 |
| | 20 | 256 | | 432 | 733 | 963 |
| | | 512 | | 329 | 560 | 736 |
| | | 1,024 | | 125 | 212 | 279 |

*With no mean stress effects

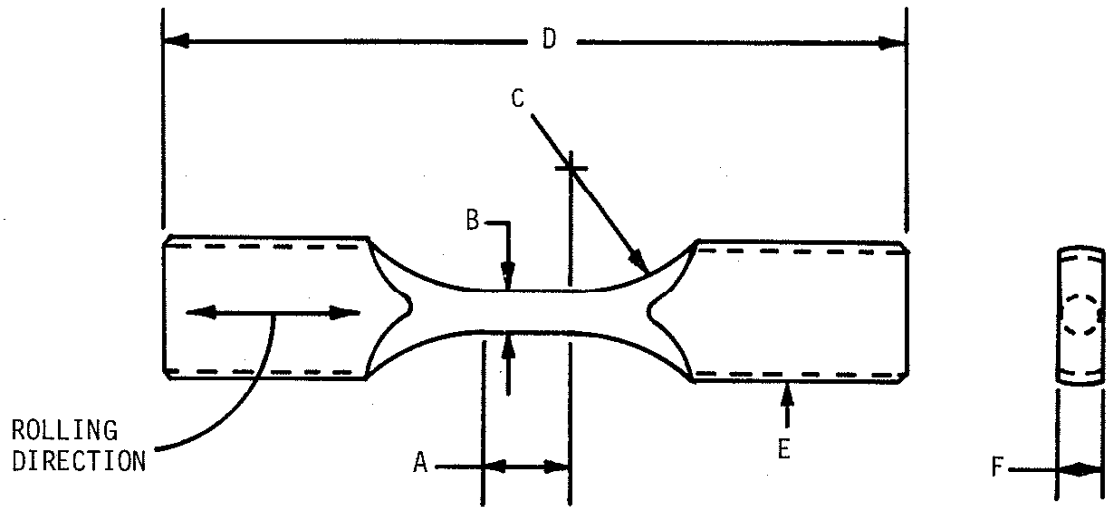


| DIMENSIONS | | | | | |
|---|---|---|---|---|---|
| GAGE LENGTH A | DIAMETER B | RADIUS C | OVERALL LENGTH D | THREAD DIAMETER E | THICKNESS F |
| 13.0 mm | 6 mm | 25 mm | 102 mm | 3/4"-16UNC | 1/4" NOM |
| 7.6 mm | 6 mm | 25 mm | 102 mm | 3/4"-16UNC | 1/4" NOM |

PROCESSING:

1) Specimens cut from as rolled 1/4" x 2" nominal HR strip stock with the rolling direction as shown.

2) Specimens machined, then polished with 1, 00, 000 emery paper successively.

3) Machined specimens stored in test tubes containing desiccant until used.

FIG. 1 SPECIMEN DIMENSIONS AND PROCESSING

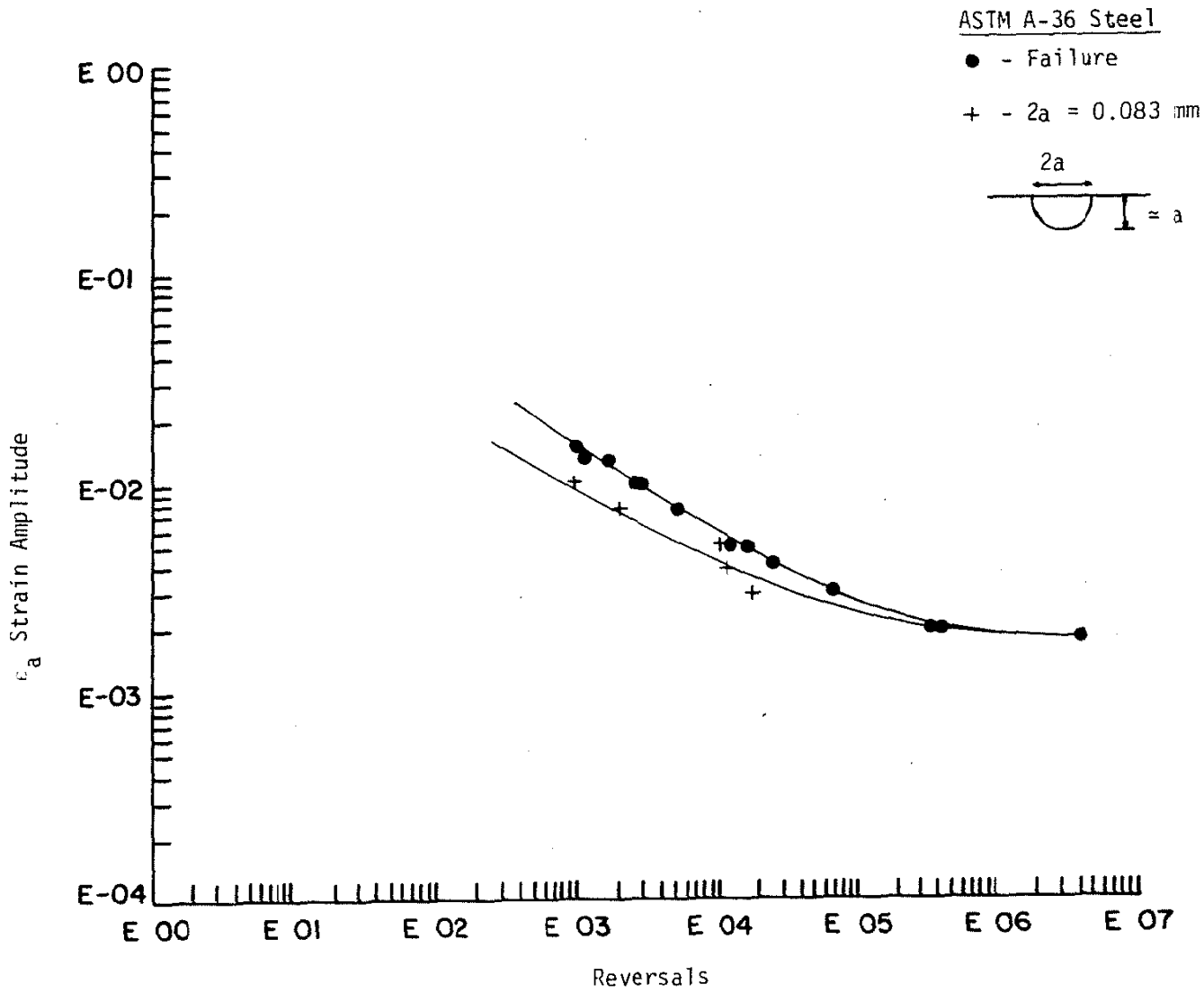


FIG. 2 CRACK LENGTH DATA

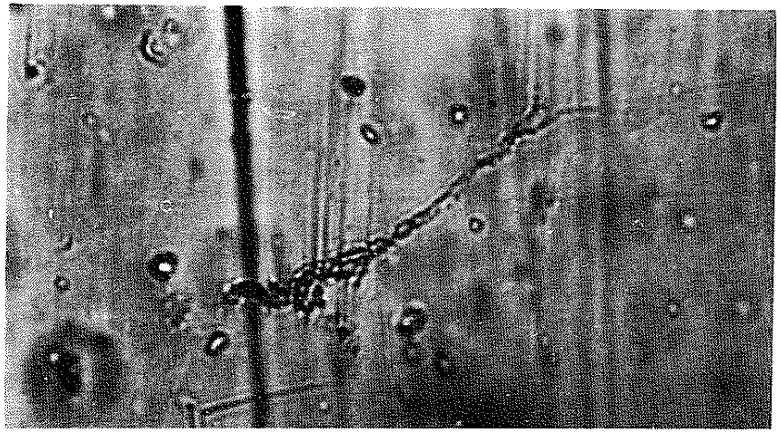

a) 24,220 REVERSALS

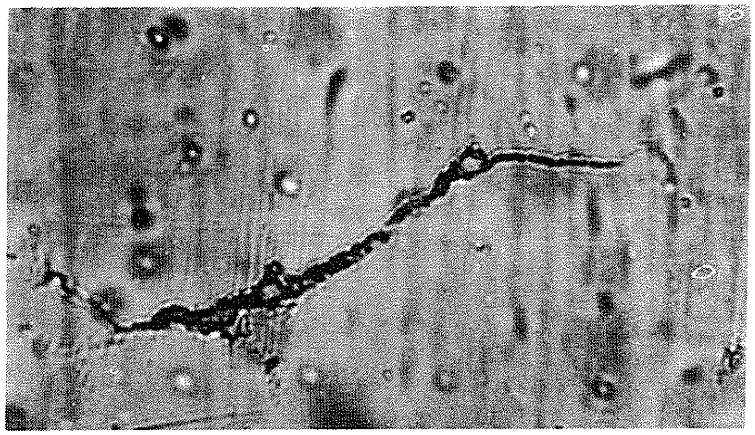

b) 32,220 REVERSALS

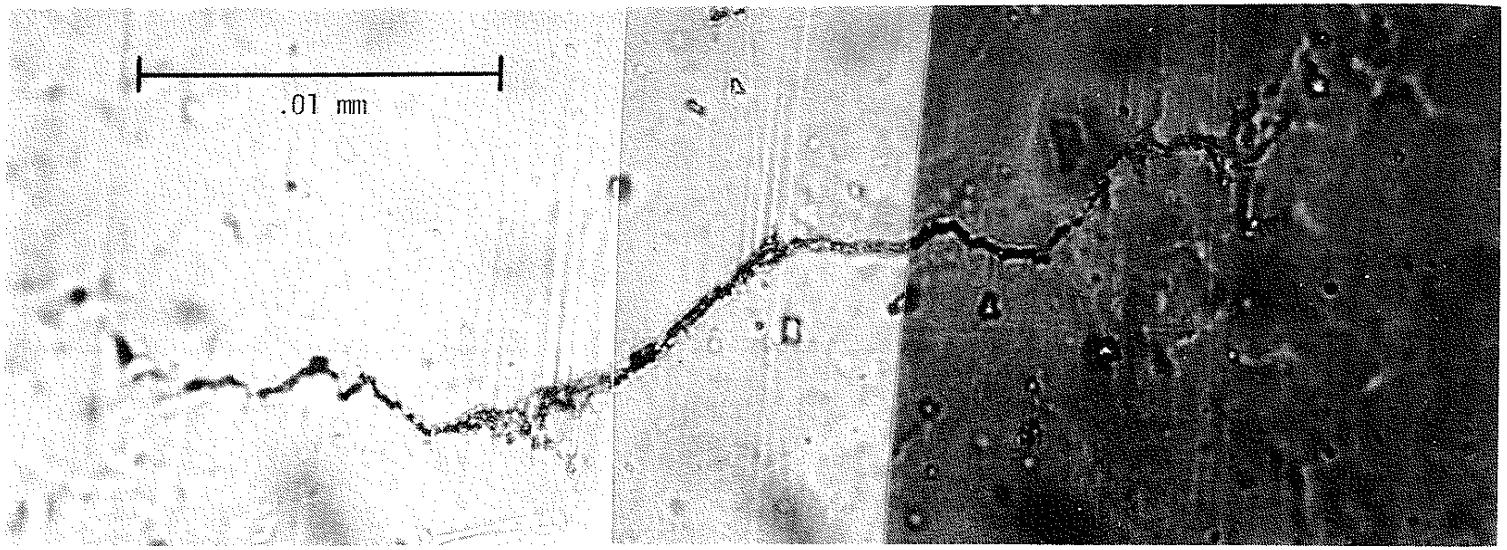


c) 40,220 REVERSALS

FIG. 3 PHOTOS OF ACETATE REPLICAS OF SPECIMEN 35A SHOWING FATIGUE CRACKS

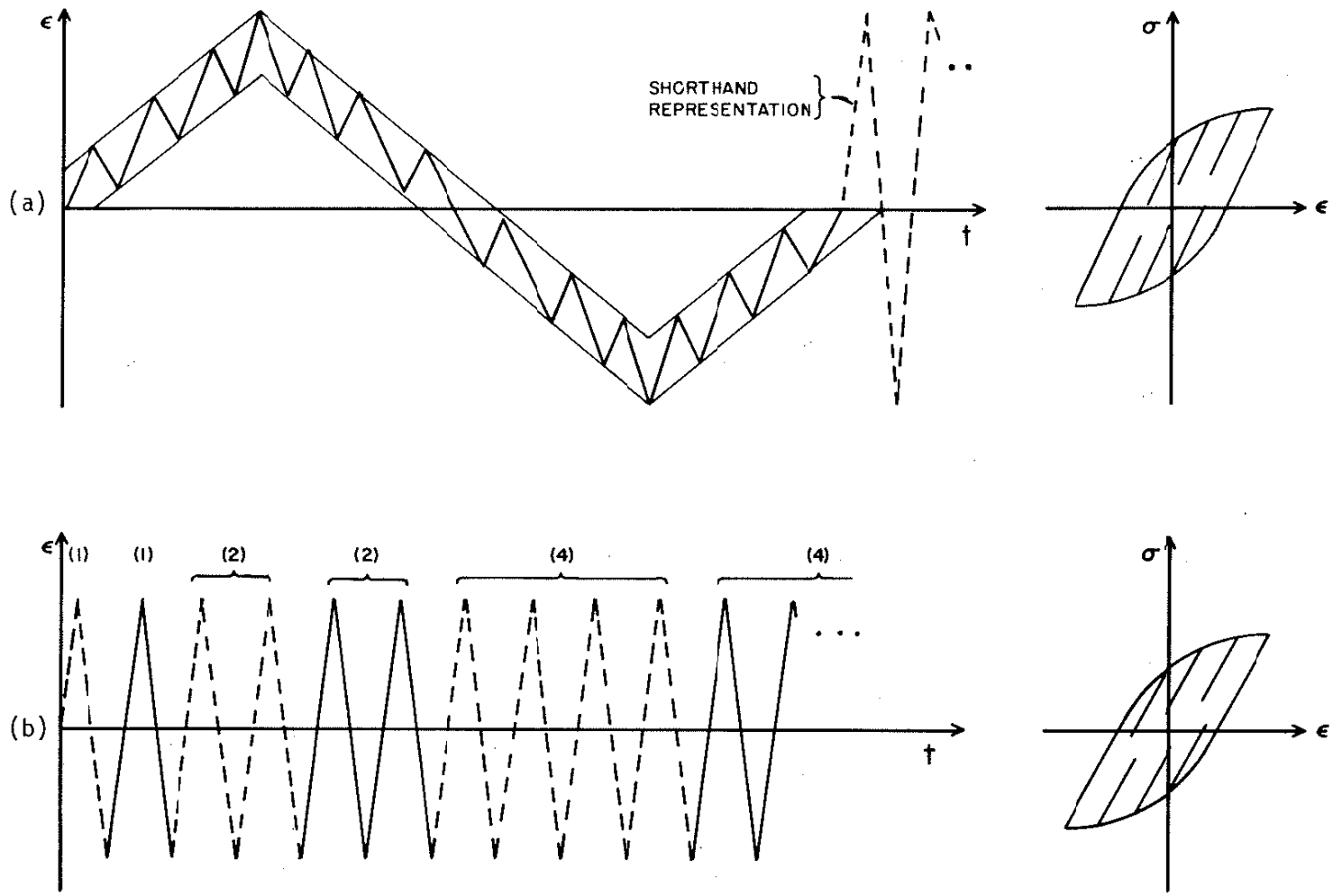


FIG. 4 SCHEMATIC ILLUSTRATION OF (a) VARYING MEAN STRESS TEST AND (b) INTERSPERSED VARYING MEAN STRESS TEST

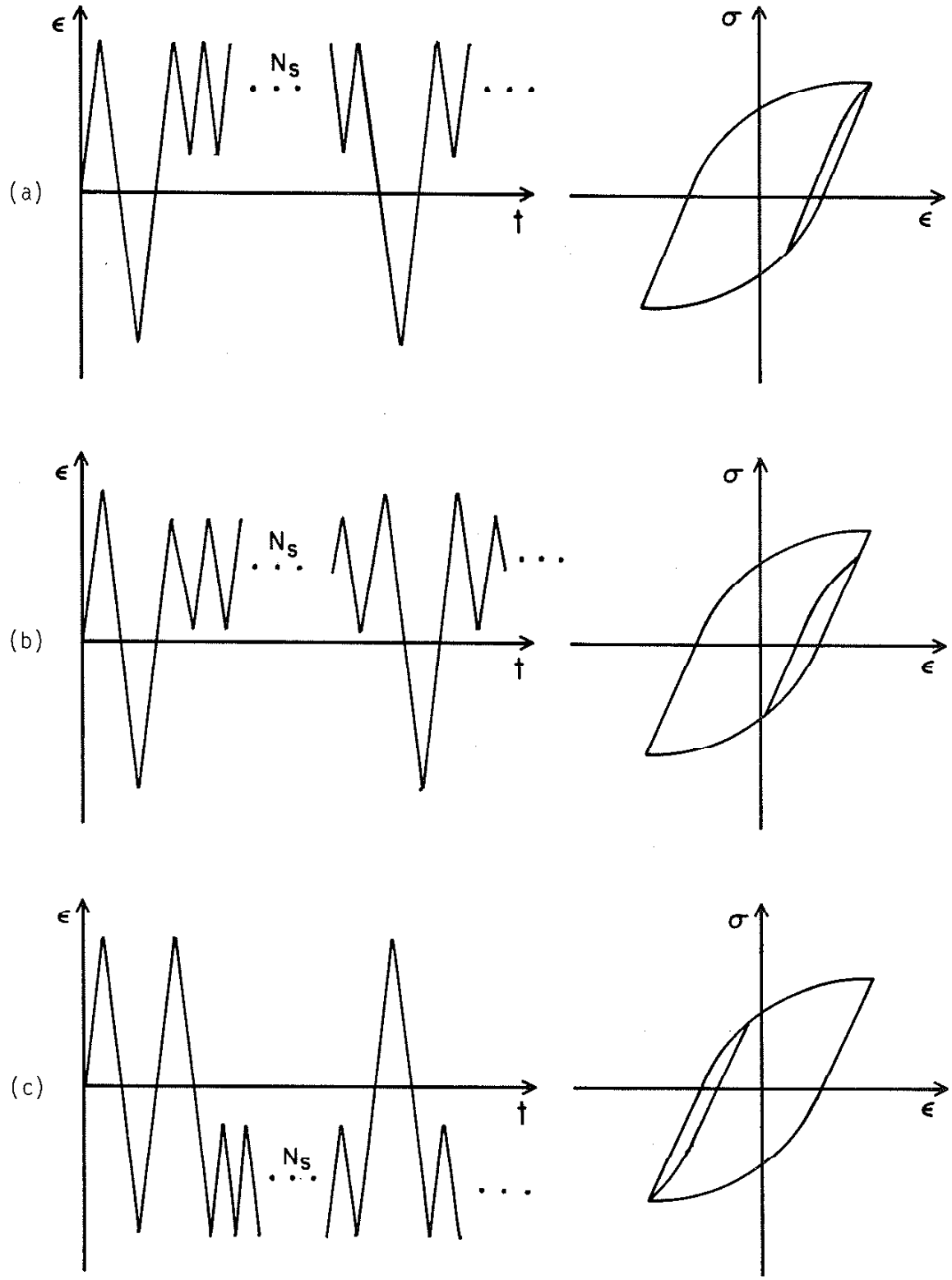


FIG. 5 SCHEMATIC REPRESENTATION OF (a) MAX MEAN STRESS TEST, (b) ZERO MEAN STRESS TEST, (c) MIN MEAN STRESS TEST

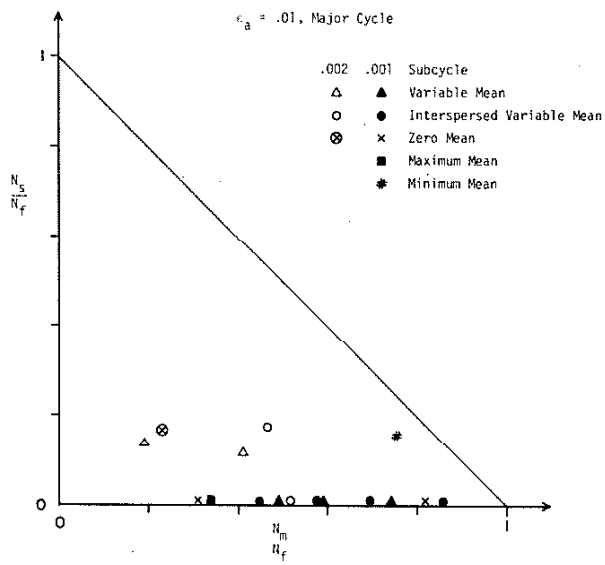


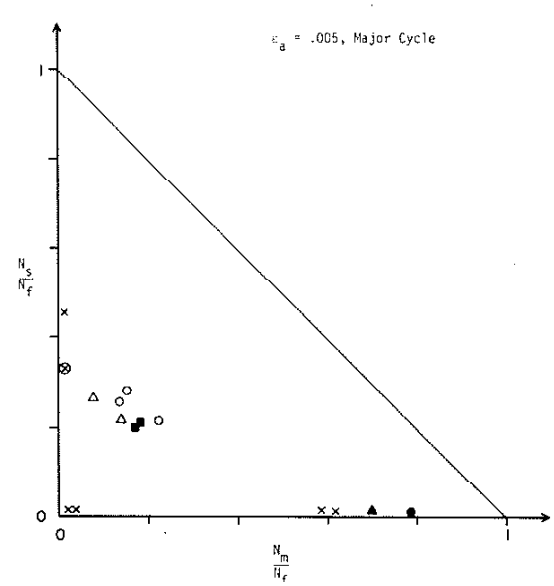


FIG. 6 EXPERIMENTAL DATA

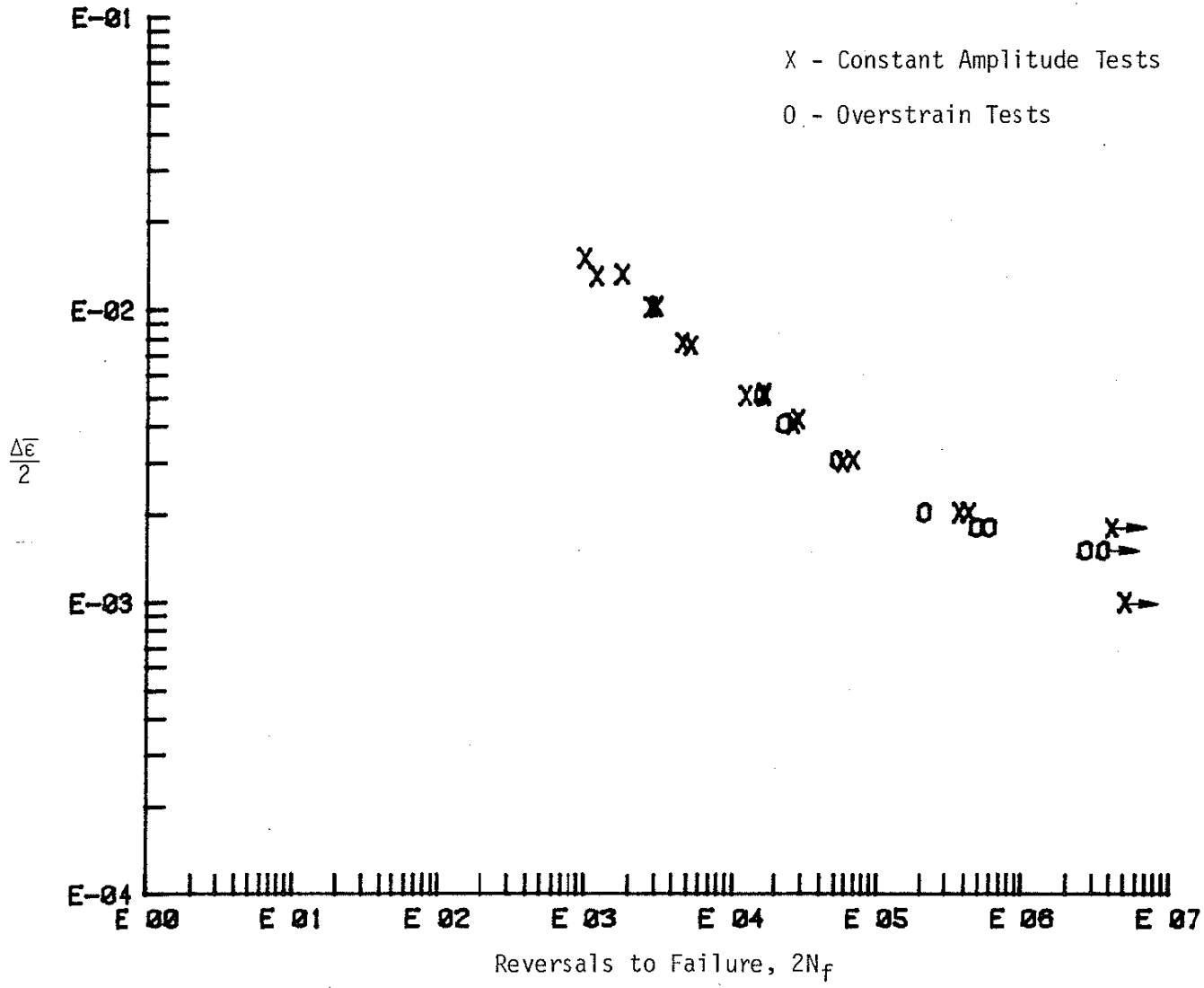


FIG. 7 COMPARISON OF CONSTANT AMPLITUDE AND OVERSTRAIN FATIGUE TESTS

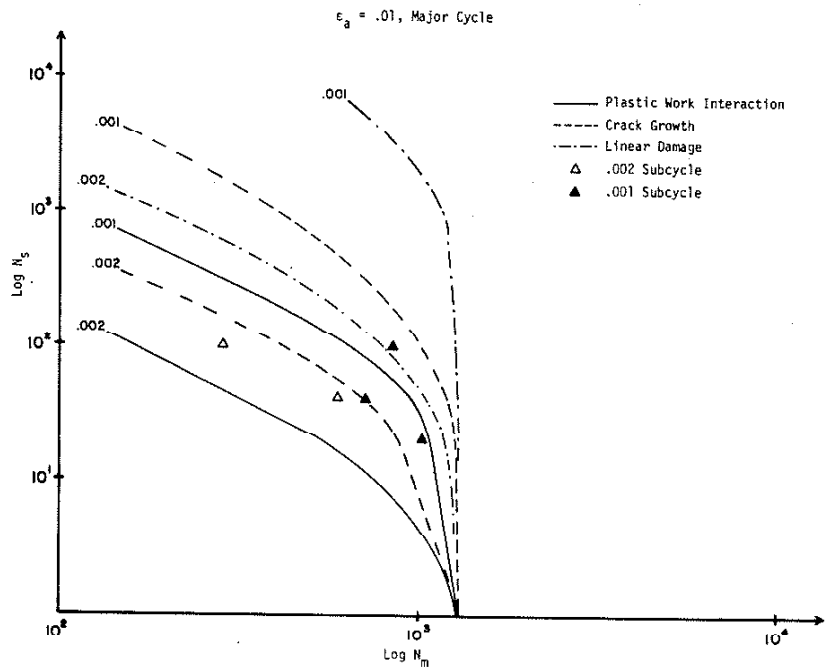


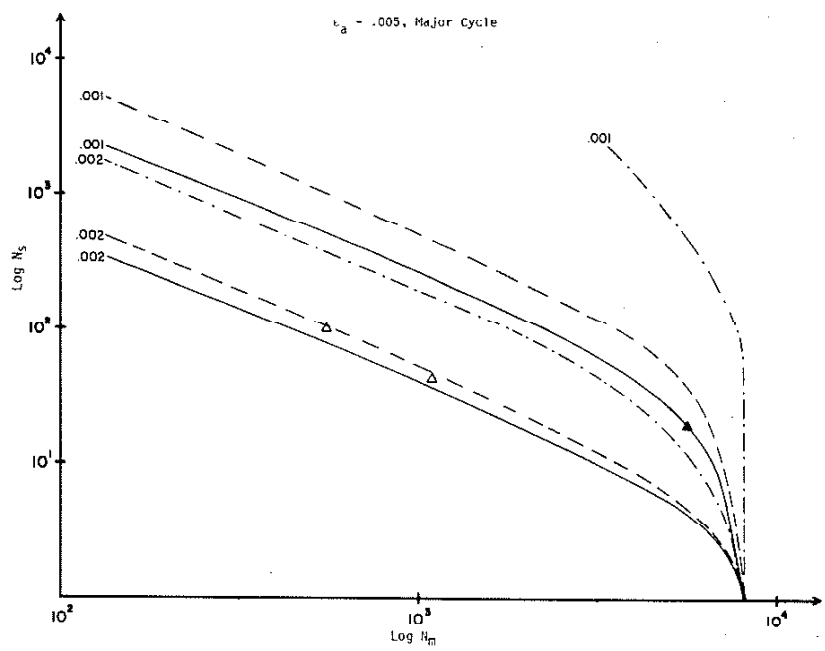


FIG. 8 PREDICTIONS AND EXPERIMENTAL RESULTS FOR THE VARYING MEAN STRESS TESTS

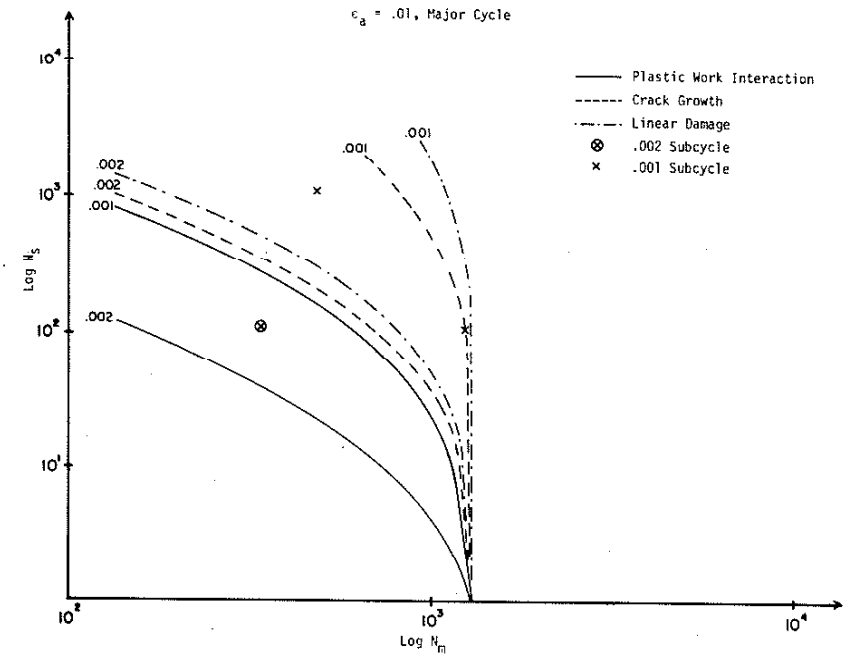


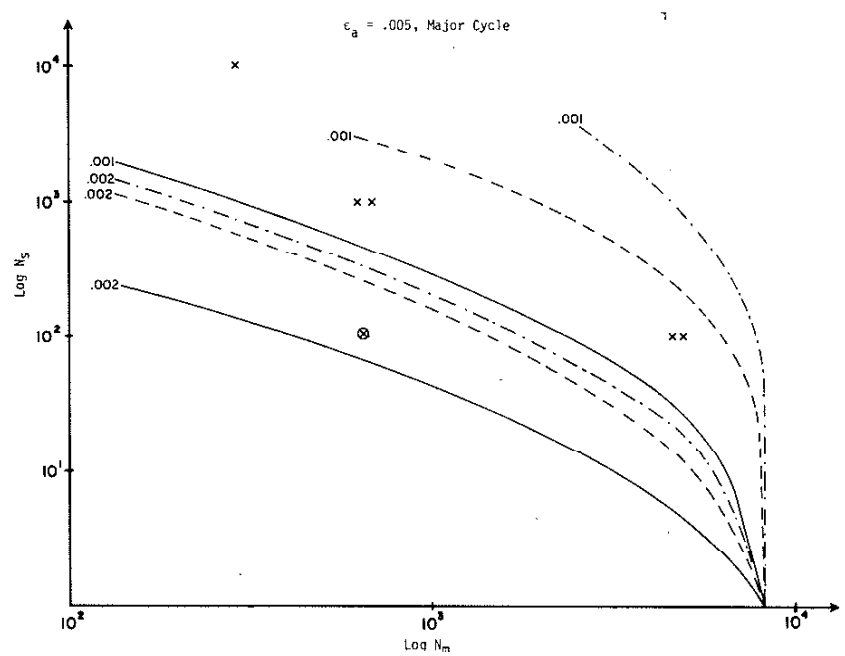


FIG. 9 PREDICTIONS AND EXPERIMENTAL RESULTS FOR THE ZERO MEAN STRESS TESTS

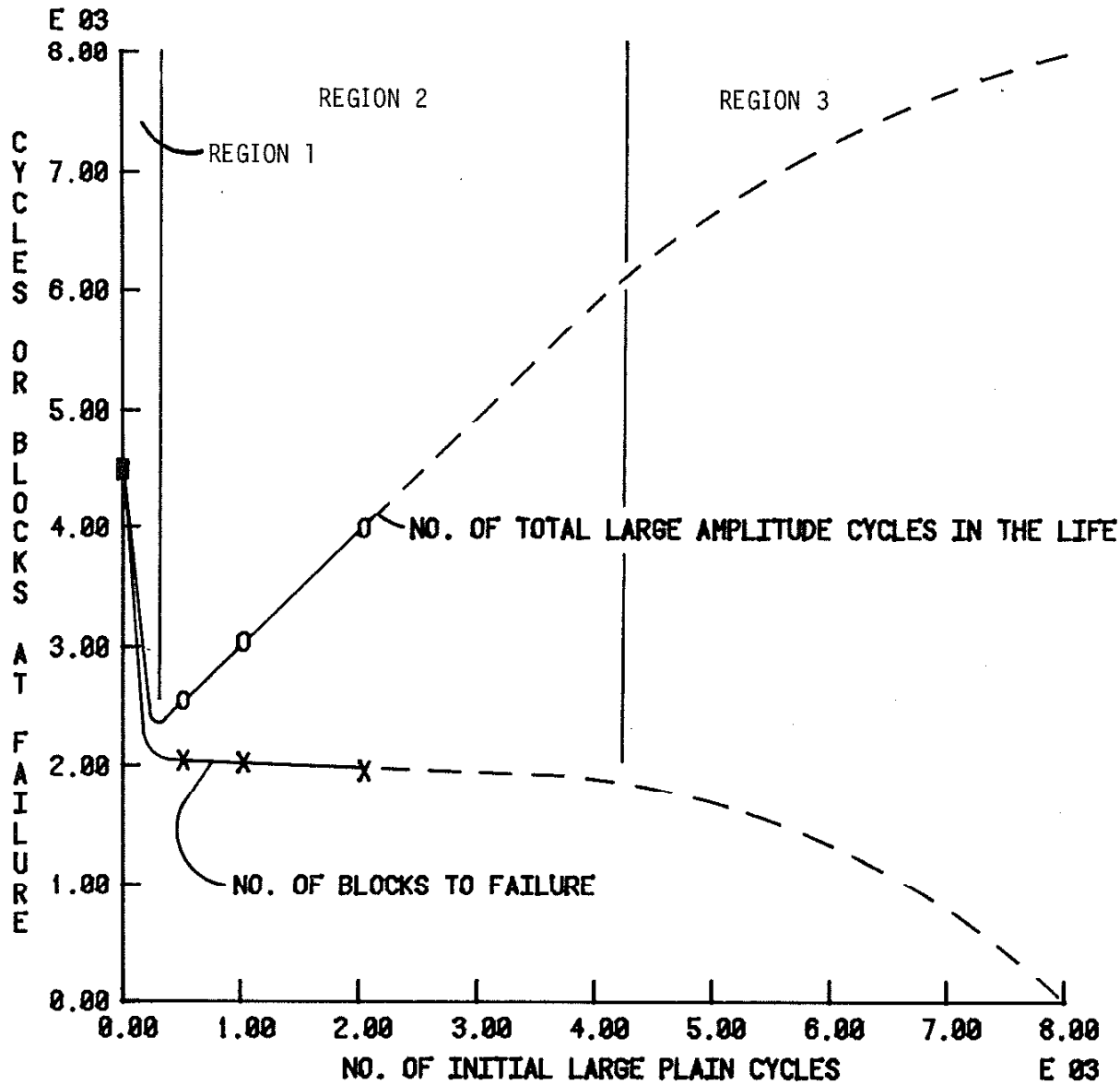


FIG. 10 LIFE VS. INITIAL PLAIN CYCLES IN EDITED VARYING MEAN STRESS

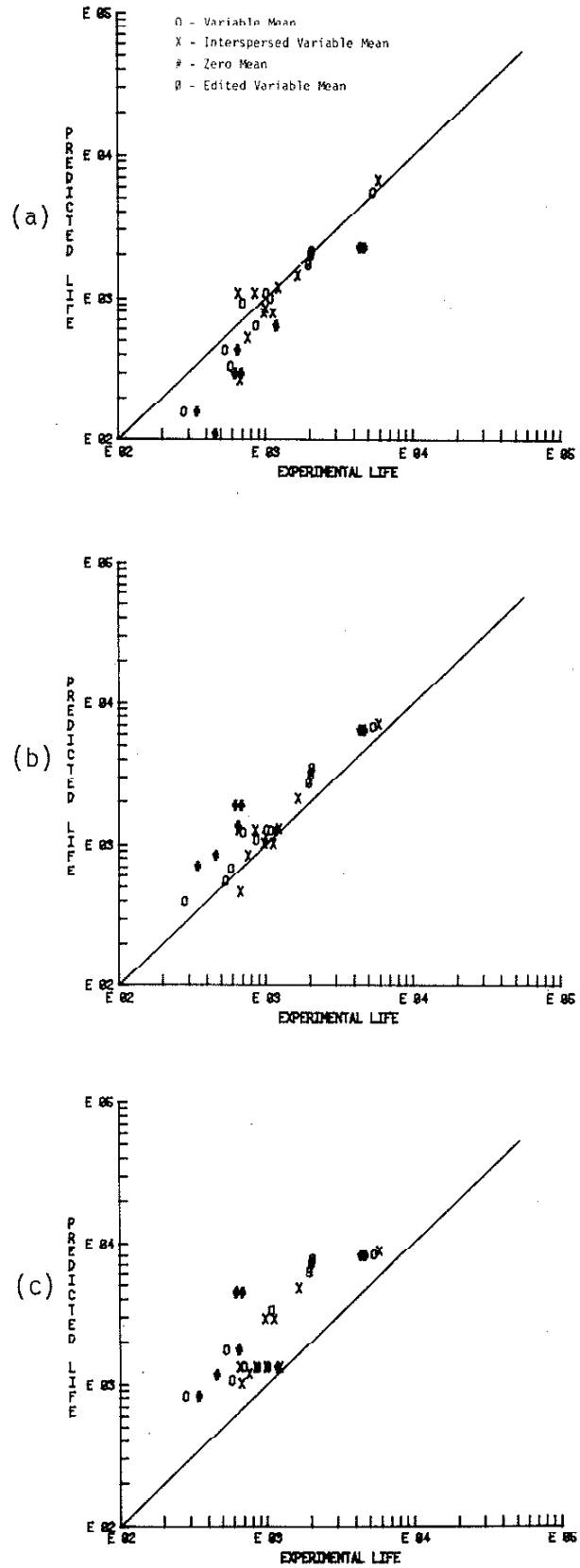


FIG. 11 PREDICTED VS. EXPERIMENTAL (a) PLASTIC WORK INTERACTION, (b) ΔJ CRACK GROWTH, (c) CONVENTIONAL LINEAR DAMAGE